

1 **Mitochondrial respiratory states and rates:**
2 **Building blocks of mitochondrial physiology Part 1**
3

4 **COST Action CA15203 MitoEAGLE preprint** Version: 2018-03-25(36)

5 Corresponding author: Gnaiger E

6 Co-authors:

7 Aasander Frostner E, Abumrad NA, Acuna-Castroviejo D, Ahn B, Ali SS, Alves MG, Amati
8 F, Aral C, Arandarčikaitė O, Bailey DM, Bajpeyi S, Bakker BM, Bastos Sant'Anna Silva AC,
9 Battino M, Bazil J, Beard DA, Bednarczyk P, Ben-Shachar D, Bergdahl A, Bernardi P,
10 Bishop D, Blier PU, Boetker HE, Boros M, Borsheim E, Borutaitė V, Bouillaud F, Boutbir J,
11 Breton S, Brown DA, Brown GC, Brown RA, Brozinick JT, Buettner GR, Burtscher J,
12 Calabria E, Calbet JA, Calzia E, Cannon DT, Canto AC, Cardoso LHD, Carvalho E, Casado
13 Pinna M, Cassina AM, Castro L, Cavalcanti-de-Albuquerque JP, Cervinkova Z, Chang SC,
14 Chaurasia B, Chen Q, Chicco AJ, Chinopoulos C, Clementi E, Coen PM, Coker RH, Collin
15 A, Crisóstomo L, Darveau CA, Das AM, Dash RK, Davis MS, De Palma C, Dembinska-Kiec
16 A, Dias TR, Distefano G, Doerrier C, Drahota Z, Dubouchaud H, Duchon MR, Dumas JF,
17 Durham WJ, Dymkowska D, Dyrstad SE, Dzialowski EM, Ehinger J, Elmer E, Endlicher R,
18 Engin AB, Fell DA, Ferko M, Ferreira JCB, Ferreira R, Fessel JP, Filipovska A, Fisar Z,
19 Fischer M, Fisher G, Fisher JJ, Fornaro M, Galkin A, Gan Z, Garcia-Roves PM, Garcia-Souza
20 LF, Garlid KD, Garrabou G, Garten A, Gastaldelli A, Genova ML, Giovarelli M, Gonzalez-
21 Armenta JL, Gonzalo H, Goodpaster BH, Gorr TA, Gourlay CW, Granata C, Grefte S, Haas
22 CB, Haavik J, Haendeler J, Hamann A, Han J, Hancock CR, Hand SC, Hargreaves I, Harrison
23 DK, Hellgren KT, Hepple RT, Hernansanz-Agustin P, Hickey AJ, Hoel F, Holland OJ,
24 Holloway GP, Hoppel CL, Houstek J, Hunger M, Iglesias-Gonzalez J, Irving BA, Iyer S,
25 Jackson CB, Jadiya P, Jang DH, Jang YC, Jansen-Dürr P, Jespersen NR, Jha RK, Jurk D,
26 Kaambre T, Kaczor JJ, Kainulainen H, Kandel SM, Kane DA, Kappler L, Karabatsiakakis A,
27 Karkucinska-Wieckowska A, Keijer J, Keppner G, Khamoui AV, Klingenspor M, Komlodi T,
28 Koopman WJH, Kopitar-Jerala N, Kowaltowski AJ, Krajcova A, Krako Jakovljevic N, Kuang
29 J, Kucera O, Kwak HB, Kwast K, Labieniec-Watala M, Lai N, Land JM, Lane N, Laner V,
30 Lanza IR, Larsen TS, Lavery GG, Lee HK, Leuwenburgh C, Lemieux H, Lerfall J, Li PA,
31 Liu J, Lucchinetti E, Macedo MP, MacMillan-Crow LA, Makrecka-Kuka M, Malik A,
32 Markova M, Martin DS, Mazat JP, McKenna HT, Menze MA, Meszaros AT, Methner A,
33 Michalak S, Moellering DR, Moiso N, Molina AJA, Montaigne D, Moreau K, Moore AL,
34 Moreira BP, Mracek T, Muntane J, Muntean DM, Murray AJ, Nair KS, Nemeč M, Neuffer
35 PD, Neuzil J, Newsom S, Nozickova K, O'Gorman D, Oliveira MF, Oliveira MT, Oliveira PF,
36 Oliveira PJ, Orynbayeva Z, Osiewacz HD, Pak YK, Pallotta ML, Palmeira CM, Parajuli N,
37 Passos JF, Patel HH, Pecina P, Pelna D, Pereira da Silva Grilo da Silva F, Pesta D, Petit
38 PX, Pettersen IKN, Pichaud N, Piel S, Pietka TA, Pino MF, Pirkmajer S, Porter C, Porter RK,
39 Pranger F, Prochownik EV, Pulinilkunnil T, Puskarich MA, Puurand M, Quijano C,
40 Radenkovic F, Radi R, Ramzan R, Rattan S, Reboredo P, Renner-Sattler K, Robinson MM,
41 Roden M, Rohlena J, Rolo AP, Ropelle ER, Røslund GV, Rossiter HB, Rybacka-
42 Mossakowska J, Saada A, Safaei Z, Salin K, Salvadego D, Sandi C, Sazanov LA, Scatena R,
43 Schartner M, Scheibye-Knudsen M, Schilling JM, Schlattner U, Schönfeld P, Schwarzer C,
44 Scott GR, Shabalina IG, Sharma P, Sharma V, Shevchuk I, Siewiera K, Silber AM, Silva AM,
45 Sims CA, Singer D, Skolik R, Smenes BT, Smith J, Soares FAA, Sobotka O, Sokolova I,
46 Sonkar VK, Sparagna GC, Sparks LM, Spinazzi M, Stankova P, Stary C, Stier A, Stocker R,
47 Sumbalova Z, Suravajhala P, Swerdlow RH, Swiniuch D, Szabo I, Szewczyk A, Tanaka M,
48 Tandler B, Tarnopolsky MA, Tavernarakis N, Tepp K, Thyfault JP, Tomar D, Towheed A,
49 Tretter L, Trifunovic A, Trivigno C, Tronstad KJ, Trougakos IP, Tyrrell DJ, Urban T,
50 Valentine JM, Velika B, Vendelin M, Vercesi AE, Victor VM, Vieyra A Villena JA, Vitorino
51 RMP, Vogt S, Volani C, Votion DM, Vujacic-Mirski K, Wagner BA, Ward ML, Warnsmann

V, Wasserman DH, Watala C, Wei YH, Wieckowski MR, Williams C, Wohlgemuth SE,
 Wohlwend M, Wolff J, Wüst RCI, Yokota T, Zablocki K, Zaugg K, Zaugg M, Zhang Y,
 Zhang YZ, Zischka H, Zorzano A

Updates and discussion:

http://www.mitoeagle.org/index.php/MitoEAGLE_preprint_2018-02-08

Correspondence: Gnaiger E

Chair COST Action CA15203 MitoEAGLE – <http://www.mitoeagle.org>

*Department of Visceral, Transplant and Thoracic Surgery, D. Swarovski Research
 Laboratory, Medical University of Innsbruck, Innrain 66/4, A-6020 Innsbruck, Austria*

Email: mitoeagle@i-med.ac.at

Tel: +43 512 566796, Fax: +43 512 566796 20

Abstract - Executive summary

1. Introduction – Box 1: In brief: Mitochondria and Bioblasts

2. Oxidative phosphorylation and coupling states in mitochondrial preparations

Mitochondrial preparations

2.1. Respiratory control and coupling

The steady-state

Specification of biochemical dose

Phosphorylation, P_{\gg} , and P_{\gg}/O_2 ratio

Control and regulation

Respiratory control and response

Respiratory coupling control and ET-pathway control

Coupling

Uncoupling

2.2. Coupling states and respiratory rates

Respiratory capacities in coupling control states

LEAK, OXPHOS, ET, ROX

Quantitative relations

2.3. Classical terminology for isolated mitochondria

States 1–5

3. Normalization: fluxes and flows

3.1. Normalization: system or sample

Flow per system, I

Extensive quantities

Size-specific quantities – Box 2: Metabolic fluxes and flows: vectorial and scalar

3.2. Normalization for system-size: flux per chamber volume

System-specific flux, J_{V,O_2}

3.3. Normalization: per sample

Sample concentration, C_{mX}

Mass-specific flux, $J_{O_2/mX}$

Number concentration, C_{NX}

Flow per object, $I_{O_2/X}$

3.4. Normalization for mitochondrial content

Mitochondrial concentration, C_{mtE} , and mitochondrial markers

Mitochondria-specific flux, $J_{O_2/mtE}$

3.5. Evaluation of mitochondrial markers

3.6. Conversion: units

4. Conclusions – Box 3: Recommendations for studies with mitochondrial preparations

References

104 **Abstract** As the knowledge base and importance of mitochondrial physiology to human health
 105 expands, the necessity for harmonizing the terminology concerning mitochondrial respiratory
 106 states and rates has become increasingly apparent. The chemiosmotic theory establishes the
 107 mechanism of energy transformation and coupling in oxidative phosphorylation. The unifying
 108 concept of the protonmotive force provides the framework for developing a consistent
 109 theoretical foundation of mitochondrial physiology and bioenergetics. We follow IUPAC
 110 guidelines on terminology in physical chemistry, extended by considerations on open systems
 111 and irreversible thermodynamics. The concept-driven constructive terminology incorporates
 112 the meaning of each quantity and aligns concepts and symbols to the nomenclature of classical
 113 bioenergetics. In the frame of COST Action MitoEAGLE open to global bottom-up input, we
 114 endeavour to provide a balanced view on mitochondrial respiratory control and a critical
 115 discussion on reporting data of mitochondrial respiration in terms of metabolic flows and fluxes.
 116 Uniform standards for evaluation of respiratory states and rates will ultimately support the
 117 development of databases of mitochondrial respiratory function in species, tissues, and cells.
 118 Clarity of concept and consistency of nomenclature facilitate effective transdisciplinary
 119 communication, education, and ultimately further discovery.

120

121 *Keywords:* Mitochondrial respiratory control, coupling control, mitochondrial
 122 preparations, protonmotive force, uncoupling, oxidative phosphorylation, OXPHOS,
 123 efficiency, electron transfer, ET; proton leak, LEAK, residual oxygen consumption, ROX, State
 124 2, State 3, State 4, normalization, flow, flux, O₂

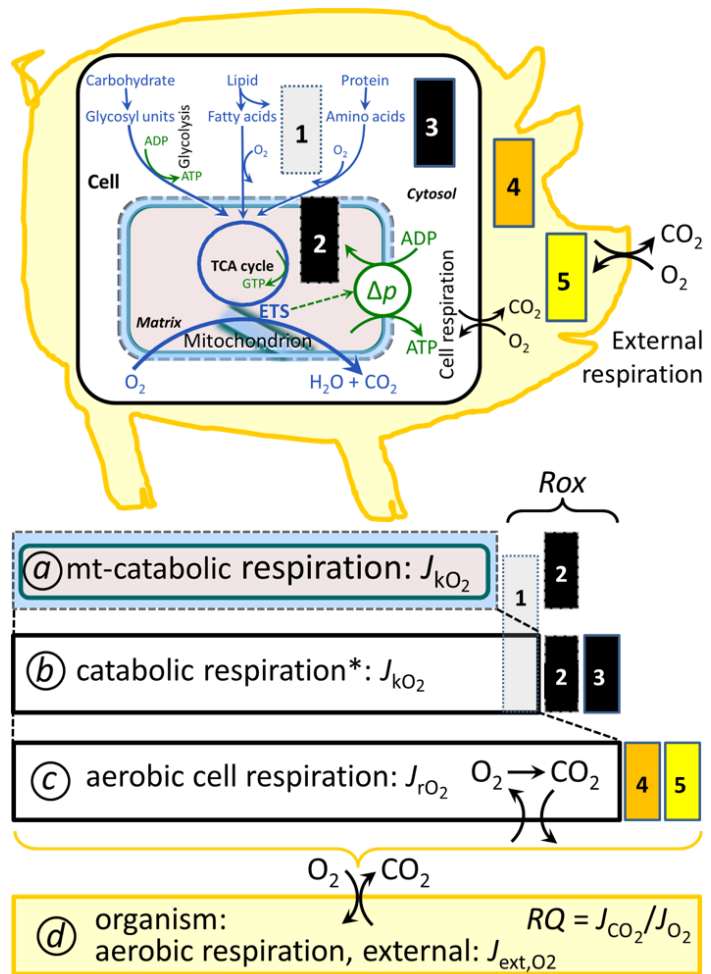
125

126 **Executive summary**

127

- 128 1. In view of the broad implications for health care, mitochondrial researchers face an
 129 increasing responsibility to disseminate their fundamental knowledge and novel
 130 discoveries to a wide range of stakeholders and scientists beyond the group of
 131 specialists. This requires implementation of a commonly accepted terminology
 132 within the discipline and standardization in the translational context. Authors,
 133 reviewers, journal editors, and lecturers are challenged to collaborate with the aim
 134 to harmonize the nomenclature in the growing field of mitochondrial physiology
 135 and bioenergetics.
- 136 2. Aerobic respiration depends on the coupling of phosphorylation (ADP → ATP) to O₂
 137 flux in catabolic reactions. Coupling in oxidative phosphorylation is mediated by
 138 translocation of protons across the inner mitochondrial membrane through proton
 139 pumps generating or utilizing the protonmotive force, that is measured between the
 140 mitochondrial matrix and intermembrane compartment or outer mitochondrial
 141 space. Compartmental coupling distinguishes vectorial oxidative phosphorylation
 142 from glycolytic fermentation as the counterpart of cellular core energy metabolism
 143 (**Figure 1**).
- 144 3. To exclude fermentation and other cytosolic interactions from exerting an effect on the
 145 analysis of mitochondrial metabolism, the barrier function of the plasma membrane
 146 must be disrupted. Selective removal or permeabilization of the plasma membrane
 147 yields mitochondrial preparations—including isolated mitochondria, tissue and
 148 cellular preparations—with structural and functional integrity. Then extra-
 149 mitochondrial concentrations of fuel substrates, ADP, ATP, inorganic phosphate,
 150 and cations including H⁺ can be controlled to determine mitochondrial function
 151 under a set of conditions defined as coupling control states. A concept-driven
 152 terminology of bioenergetics explicitly incorporates in its terms and symbols
 153 information on the nature of respiratory states that makes the technical terms readily
 154 recognized and more easy to understand.

155 **Figure 1. Mitochondrial respiration**
 156 **is the oxidation of fuel substrates**
 157 **(electron donors) and reduction of**
 158 **O₂ catalysed by the electron**
 159 **transfer system, ETS: (a)**
 160 **mitochondrial catabolic**
 161 **respiration; (b) mitochondrial and**
 162 **non-mitochondrial catabolic O₂**
 163 **consumption; O₂ balance of (c) total**
 164 **cellular O₂ consumption and (d)**
 165 **external respiration**



166 All chemical reactions, r , that
 167 consume O₂ in the cells of an
 168 organism, contribute to cell
 169 respiration, J_{rO_2} . ❶ Non-mitochondrial
 170 O₂ consumption by catabolic
 171 reactions, particularly peroxisomal
 172 oxidases; ❷ mitochondrial residual
 173 oxygen consumption, Rox , after
 174 blocking the ETS; ❸ non-
 175 mitochondrial Rox ; ❹ extracellular O₂
 176 consumption; ❺ aerobic microbial
 177 respiration. Bars are not at a
 178 quantitative scale.

179 **a Mitochondrial catabolic**
 180 **respiration, J_{kO_2} , is the O₂**
 181 **consumption by the mitochondrial**
 182 **ETS maintaining the protonmotive force, Δp . J_{kO_2} excludes Rox .**

183 **b Catabolic respiration** is the O₂ consumption associated with catabolic pathways in the cell,
 184 including peroxisomal oxidation reactions (❶) in addition to mitochondrial catabolism (*
 185 The reactions k have to be defined specifically for *a* and *b*.)

186 **c Aerobic cell respiration, J_{rO_2} , takes into account internal O₂-consuming reactions, r ,**
 187 **including catabolic respiration and Rox . Internal respiration of an organism includes**
 188 **extracellular O₂ consumption (❹) and aerobic respiration by the microbiome (❺).**
 189 **Respiration is distinguished from fermentation by: (1) External electron acceptors for the**
 190 **maintenance of redox balance, whereas fermentation is characterized by an internal electron**
 191 **acceptor produced in intermediary metabolism. In aerobic cell respiration, redox balance is**
 192 **maintained by O₂ as the electron acceptor. (2) Compartmental coupling in vectorial oxidative**
 193 **phosphorylation, in contrast to exclusively scalar substrate-level phosphorylation in**
 194 **fermentation.**

195 **d External respiration** balances internal respiration at steady-state. O₂ is transported from the
 196 environment across the respiratory cascade (circulation between tissues and diffusion across
 197 cell membranes) to the intracellular compartment, while bicarbonate and CO₂ are transported
 198 in reverse to the extracellular milieu and the organismic environment. Hemoglobin provides
 199 the molecular paradigm for the combination of O₂ and CO₂ exchange, as do lungs and gills
 200 on the morphological level. The respiratory quotient, RQ , is the molar CO₂/O₂ exchange
 201 ratio; when combined with the respiratory nitrogen quotient, N/O₂ (mol N given off per mol
 202 O₂ consumed), the RQ reflects the proportion of carbohydrate, lipid and protein utilized in
 203 cell respiration during aerobically balanced steady-states.

204

- 205 4. Mitochondrial coupling states are defined according to the control of respiratory oxygen
 206 flux by the protonmotive force. Capacities of oxidative phosphorylation and
 207 electron transfer are measured at kinetically saturating concentrations of fuel
 208 substrates, ADP and inorganic phosphate, or at optimal uncoupler concentrations,
 209 respectively. Respiratory capacity is a measure of the upper bound of the rate of
 210 respiration, depends on the substrate type undergoing oxidation, and provides
 211 reference values for the diagnosis of health and disease, and for evaluation of the
 212 effects of Evolutionary background, Age, Gender and sex, Lifestyle and
 213 Environment (EAGLE).
- 214 5. Incomplete tightness of coupling, *i.e.*, some degree of uncoupling relative to the
 215 substrate-dependent coupling stoichiometry, is a characteristic of energy-
 216 transformations across membranes. Uncoupling is caused by a variety of
 217 physiological, pathological, toxicological, pharmacological and environmental
 218 conditions that exert an influence not only on the proton leak and cation cycling,
 219 but also on proton slip within the proton pumps and the structural integrity of the
 220 mitochondria. A more loosely coupled state is induced by stimulation of
 221 mitochondrial superoxide formation and the bypass of proton pumps. In addition,
 222 uncoupling by application of protonophores represents an experimental
 223 intervention for the transition from a well-coupled to the noncoupled state of
 224 mitochondrial respiration.
- 225 6. Respiratory oxygen consumption rates have to be carefully normalized to enable meta-
 226 analytic studies beyond the specific question of a particular experiment. Therefore,
 227 all raw data should be published in a supplemental table or open access data
 228 repository. Normalization of rates for the volume of the experimental chamber (the
 229 measuring system) is distinguished from normalization for: (1) the volume or mass
 230 of the experimental sample; (2) the number of objects (cells, organisms); and (3)
 231 the concentration of mitochondrial markers in the chamber.
- 232 7. The consistent use of terms and symbols will facilitate transdisciplinary communication
 233 and support further developments of a database on bioenergetics and mitochondrial
 234 physiology. The present considerations are focused on studies with mitochondrial
 235 preparations. These will be extended in a series of reports on pathway control of
 236 mitochondrial respiration, the protonmotive force, respiratory states in intact cells,
 237 and harmonization of experimental procedures.
 238

239
 240

241 **Box 1: In brief – Mitochondria and Bioblasts**

242 *‘For the physiologist, mitochondria afforded the first opportunity for an*
 243 *experimental approach to structure-function relationships, in particular those*
 244 *involved in active transport, vectorial metabolism, and metabolic control*
 245 *mechanisms on a subcellular level’ (Ernster and Schatz 1981).*

246 **Mitochondria** are the oxygen-consuming electrochemical generators evolved from
 247 endosymbiotic bacteria (Margulis 1970; Lane 2005). They were described by Richard Altmann
 248 (1894) as ‘bioblasts’, which include not only the mitochondria as presently defined, but also
 249 symbiotic and free-living bacteria. The word ‘mitochondria’ (Greek mitos: thread; chondros:
 250 granule) was introduced by Carl Benda (1898).

251 Mitochondria form dynamic networks within eukaryotic cells and are morphologically
 252 enclosed by a double membrane. The mitochondrial inner membrane (mtIM) shows dynamic
 253 tubular to disk-shaped cristae that separate the mitochondrial matrix, *i.e.*, the negatively charged
 254 internal mitochondrial compartment, from the intermembrane space; the latter being enclosed
 255 by the mitochondrial outer membrane (mtOM) and positively charged with respect to the
 256 matrix. The mtIM contains the non-bilayer phospholipid cardiolipin, which is not present in

257 any other eukaryotic cellular membrane. Cardiolipin stabilizes and promotes the formation of
258 respiratory supercomplexes (SC I_nIII_nIV_n), which are supramolecular assemblies based upon
259 specific, though dynamic interactions between individual respiratory complexes (Greggio *et al.*
260 2017; Lenaz *et al.* 2017). Membrane fluidity exerts an influence on functional properties of
261 proteins incorporated in the membranes (Waczulikova *et al.* 2007). In addition to mitochondrial
262 movement along microtubules, mitochondrial morphology can change in response to energy
263 requirements of the cell via processes known as fusion and fission, through which mitochondria
264 communicate within a network. Intracellular stress factors may cause shrinking or swelling of
265 the mitochondrial matrix, which can ultimately result in permeability transition.

266 Mitochondria are the structural and functional elements of cell respiration. Mitochondrial
267 respiration is the reduction of oxygen by electron transfer coupled to electrochemical proton
268 translocation across the mtIM. In the process of oxidative phosphorylation (OXPHOS), the
269 catabolic reaction of oxygen consumption is electrochemically coupled to the transformation of
270 energy in the form of adenosine triphosphate (ATP; Mitchell 1961, 2011). Mitochondria are the
271 powerhouses of the cell which contain the machinery of the OXPHOS-pathways, including
272 transmembrane respiratory complexes (proton pumps with FMN, Fe-S and cytochrome *b*, *c*,
273 *aa*₃ redox systems); alternative dehydrogenases and oxidases; the coenzyme ubiquinone (Q);
274 F-ATPase or ATP synthase; the enzymes of the tricarboxylic acid cycle, fatty acid and amino
275 acid oxidation; transporters of ions, metabolites and co-factors; iron/sulphur cluster synthesis;
276 and mitochondrial kinases related to energy transfer pathways. The mitochondrial proteome
277 comprises over 1,200 proteins (Calvo *et al.* 2015; 2017), mostly encoded by nuclear DNA
278 (nDNA), with a variety of functions, many of which are relatively well known (*e.g.*, proteins
279 regulating mitochondrial biogenesis or apoptosis), while others are still under investigation, or
280 need to be identified (*e.g.*, alanine transporter). Only lately it is possible to use the mammalian
281 mitochondrial proteome to discover and characterize the genetic basis of mitochondrial diseases
282 (Williams *et al.* 2016; Palmfeldt and Bross 2017).

283 There is a constant crosstalk between mitochondria and the other cellular components.
284 The crosstalk between mitochondria and endoplasmic reticulum is involved in the regulation of
285 calcium homeostasis, cell division, autophagy, differentiation, and anti-viral signaling (Murley
286 and Nunnari 2016). Mitochondria contribute to the formation of peroxisomes, which are hybrids
287 of mitochondrial and ER-derived precursors (Sugiura *et al.* 2017). Cellular mitochondrial
288 homeostasis (mitostasis) is maintained through regulation at both the transcriptional and post-
289 translational level. Cell signalling modules contribute to homeostatic regulation throughout the
290 cell cycle or even cell death by activating proteostatic modules (*e.g.*, the ubiquitin-proteasome
291 and autophagy-lysosome/vacuole pathways; specific proteases like LON) and genome stability
292 modules in response to varying energy demands and stress cues (Quiros *et al.* 2016).
293 Acetylation is a post-translational modification capable of influencing the bioenergetic
294 response, with clinically significant implications for health and disease (Carrico *et al.* 2018).
295 Mitochondria can traverse cell boundaries in a process known as horizontal mitochondrial
296 transfer (Torralba *et al.* 2016).

297 Mitochondria typically maintain several copies of their own circular genome known as
298 mitochondrial DNA (mtDNA; hundred to thousands per cell; Cummins 1998), which is
299 maternally inherited. Biparental mitochondrial inheritance is documented in mammals, birds,
300 fish, reptiles and invertebrate groups, and is even the norm in bivalves (Breton *et al.* 2007;
301 White *et al.* 2008). The mitochondrial genome of the angiosperm *Amborella* contains a record
302 of six mitochondrial genome equivalents acquired by horizontal transfer of entire genomes, two
303 from angiosperms, three from algae and one from mosses (Rice *et al.* 2016). However, some
304 organisms such as *Cryptosporidium* species have morphologically and functionally reduced
305 mitochondria without DNA (Liu *et al.* 2016). mtDNA is compact (16.5 kB in humans) and
306 encodes 13 protein subunits of the transmembrane respiratory Complexes CI, CIII, CIV and F-
307 ATPase, 22 tRNAs, and two RNAs. Additional gene content has been suggested to include

308 microRNAs, piRNA, smithRNAs, repeat associated RNA, and even additional proteins (Duarte
309 *et al.* 2014; Lee *et al.* 2015; Cobb *et al.* 2016). The mitochondrial genome requires nuclear-
310 encoded mitochondrially targeted proteins for its maintenance and expression (Rackham *et al.*
311 2012).

312 Mitochondrial dysfunction is associated with a wide variety of genetic and degenerative
313 diseases. Robust mitochondrial function is supported by physical exercise and caloric balance,
314 and is central for sustained metabolic health throughout life. Therefore, a more consistent
315 presentation of mitochondrial physiology will improve our understanding of the etiology of
316 disease, the diagnostic repertoire of mitochondrial medicine, with a focus on protective
317 medicine, lifestyle and healthy aging.

318 Abbreviation: mt, as generally used in mtDNA. Mitochondrion is singular and
319 mitochondria is plural.

321

322

323 1. Introduction

324

325 Mitochondria are the powerhouses of the cell with numerous physiological, molecular,
326 and genetic functions (**Box 1**). Every study of mitochondrial health and disease is faced with
327 **E**volution, **A**ge, **G**ender and sex, **L**ifestyle, and **E**nvironment (EAGLE) as essential background
328 conditions intrinsic to the individual person or cohort, species, tissue and to some extent even
329 cell line. As a large and coordinated group of laboratories and researchers, the mission of the
330 global MitoEAGLE Network is to generate the necessary scale, type, and quality of consistent
331 data sets and conditions to address this intrinsic complexity. Harmonization of experimental
332 protocols and implementation of a quality control and data management system are required to
333 interrelate results gathered across a spectrum of studies and to generate a rigorously monitored
334 database focused on mitochondrial respiratory function. In this way, researchers from a variety
335 of disciplines can compare their findings using clearly defined and accepted international
336 standards.

337 Reliability and comparability of quantitative results depend on the accuracy of
338 measurements under strictly-defined conditions. A conceptual framework is required to warrant
339 meaningful interpretation and comparability of experimental outcomes carried out by research
340 groups at different institutes. With an emphasis on quality of research, collected data can be
341 useful far beyond the specific question of a particular experiment. Standardization and
342 homogenization of terminology, methodology, and data sets could lead to the development of
343 open-access databases such as those that have been developed for National Institutes of Health
344 sponsored research in genetics, proteomics, and metabolomics. Enabling meta-analytic studies
345 is the most economic way of providing robust answers to biological questions (Cooper *et al.*
346 2009). Vague or ambiguous jargon can lead to confusion and may relegate valuable signals to
347 wasteful noise. For this reason, measured values must be expressed in standard units for each
348 parameter used to define mitochondrial respiratory function. Harmonization of nomenclature
349 and definition of technical terms are essential to improve the awareness of the intricate meaning
350 of current and past scientific vocabulary, for documentation and integration into databases in
351 general, and quantitative modelling in particular (Beard 2005). The focus on coupling states
352 and fluxes through metabolic pathways of aerobic energy transformation in mitochondrial
353 preparations is a first step in the attempt to generate a conceptually-oriented nomenclature in
354 bioenergetics and mitochondrial physiology. Coupling states of intact cells, the protonmotive
355 force, and respiratory control by fuel substrates and specific inhibitors of respiratory enzymes
356 will be reviewed in subsequent communications.

357

358

2. Oxidative phosphorylation and coupling states in mitochondrial preparations

‘Every professional group develops its own technical jargon for talking about matters of critical concern ... People who know a word can share that idea with other members of their group, and a shared vocabulary is part of the glue that holds people together and allows them to create a shared culture’ (Miller 1991).

Mitochondrial preparations are defined as either isolated mitochondria, or tissue and cellular preparations in which the barrier function of the plasma membrane is disrupted. Since this entails the loss of cell viability, mitochondrial preparations are not studied *in vivo*. In contrast to isolated mitochondria and tissue homogenate preparations, mitochondria in permeabilized tissues and cells are *in situ* relative to the plasma membrane. The plasma membrane separates the intracellular compartment including the cytosol, nucleus, and organelles from the environment of the cell. The plasma membrane consists of a lipid bilayer with embedded proteins and attached organic molecules that collectively control the selective permeability of ions, organic molecules, and particles across the cell boundary. The intact plasma membrane prevents the passage of many water-soluble mitochondrial substrates and inorganic ions—such as succinate, adenosine diphosphate (ADP) and inorganic phosphate (P_i), that must be controlled at kinetically-saturating concentrations for the analysis of respiratory capacities. Despite of the possible presence of solute carriers that transport these metabolites across the cell membrane, *e.g.*, SLC13A3 and SLC20A2, this limits the scope of investigations into mitochondrial respiratory function in intact cells (**Figure 2A**).

The cholesterol content of the plasma membrane is high compared to mitochondrial membranes. Therefore, mild detergents—such as digitonin and saponin—can be applied to selectively permeabilize the plasma membrane by interaction with cholesterol and allow free exchange of organic molecules and inorganic ions between the cytosol and the immediate cell environment, while maintaining the integrity and localization of organelles, cytoskeleton, and the nucleus. Application of optimum concentrations of permeabilization agents (mild detergents or toxins) leads to washout of cytosolic marker enzymes—such as lactate dehydrogenase—and results in the complete loss of cell viability, tested by nuclear staining using membrane-impermeable dyes, while mitochondrial function remains intact. Respiration of isolated mitochondria remains unaltered after the addition of low concentrations of digitonin or saponin. In addition to mechanical cell disruption during homogenization of tissue, permeabilization agents may be applied to ensure permeabilization of all cells. Suspensions of cells permeabilized in the respiration chamber and crude tissue homogenates contain all components of the cell at highly dilute concentrations. All mitochondria are retained in chemically-permeabilized mitochondrial preparations and crude tissue homogenates. In the preparation of isolated mitochondria, the cells or tissues are homogenized, and the mitochondria are separated from other cell fractions and purified by differential centrifugation, entailing the loss of a fraction of the total mitochondrial content. Typical mitochondrial recovery ranges from 30% to 80%. Using Percoll or sucrose density gradients to maximize the purity of isolated mitochondria may compromise the mitochondrial yield or structural and functional integrity. Therefore, protocols to isolate mitochondria need to be optimized according to each study. The term mitochondrial preparation does neither include further fractionation of mitochondrial components, nor submitochondrial particles.

2.1. Respiratory control and coupling

Respiratory coupling control states are established in studies of mitochondrial preparations to obtain reference values for various output variables. Physiological conditions *in vivo* deviate from these experimentally obtained states. Since kinetically-saturating concentrations, *e.g.*, of ADP or oxygen (O_2 ; dioxygen), may not apply to physiological

410 intracellular conditions, relevant information is obtained in studies of kinetic responses to
 411 variations in [ADP] or [O₂] in the range between kinetically-saturating concentrations and
 412 anoxia (Gnaiger 2001).

413 **The steady-state:** Mitochondria represent a thermodynamically open system in non-
 414 equilibrium states of biochemical energy transformation. State variables (protonmotive force;
 415 redox states) and metabolic *rates* (fluxes) are measured in defined mitochondrial respiratory
 416 *states*. Steady-states can be obtained only in open systems, in which changes by *internal*
 417 transformations, *e.g.*, O₂ consumption, are instantaneously compensated for by *external* fluxes,
 418 *e.g.*, O₂ supply, preventing a change of O₂ concentration in the system (Gnaiger 1993b).
 419 Mitochondrial respiratory states monitored in closed systems satisfy the criteria of pseudo-
 420 steady states for limited periods of time, when changes in the system (concentrations of O₂, fuel
 421 substrates, ADP, P_i, H⁺) do not exert significant effects on metabolic fluxes (respiration,
 422 phosphorylation). Such pseudo-steady states require respiratory media with sufficient buffering
 423 capacity and substrates maintained at kinetically-saturating concentrations, and thus depend on
 424 the kinetics of the processes under investigation.

425 **Specification of biochemical dose:** Substrates, uncouplers, inhibitors, and other
 426 chemical reagents are titrated to dissect mitochondrial function. Nominal concentrations of
 427 these substances are usually reported as initial amount of substance concentration [mol·L⁻¹] in
 428 the incubation medium. When aiming at the measurement of kinetically saturated processes—
 429 such as OXPHOS-capacities, the concentrations for substrates can be chosen according to the
 430 apparent equilibrium constant, K_m' . In the case of hyperbolic kinetics, only 80% of maximum
 431 respiratory capacity is obtained at a substrate concentration of four times the K_m' , whereas
 432 substrate concentrations of 5, 9, 19 and 49 times the K_m' are theoretically required for reaching
 433 83%, 90%, 95% or 98% of the maximal rate (Gnaiger 2001). Other reagents are chosen to
 434 inhibit or alter some processes. The amount of these chemicals in an experimental incubation
 435 is selected to maximize effect, avoiding unacceptable off-target consequences that would
 436 adversely affect the data being sought. Specifying the amount of substance in an incubation as
 437 nominal concentration in the aqueous incubation medium can be ambiguous (Doskey *et al.*
 438 2015), particularly for lipophilic substances (oligomycin, uncouplers, permeabilization agents)
 439 or cations (TPP⁺; fluorescent dyes such as safranin, TMRM), which accumulate in biological
 440 membranes or in the mitochondrial matrix. For example, a dose of digitonin of 8 fmol·cell⁻¹ (10
 441 pg·cell⁻¹; 10 μg·10⁻⁶ cells) is optimal for permeabilization of endothelial cells, and the
 442 concentration in the incubation medium has to be adjusted according to the cell density applied
 443 (Doerrier *et al.* 2018).

444 Generally, dose/exposure can be specified per unit of biological sample, *i.e.*, (nominal
 445 moles of xenobiotic)/(number of cells) [mol·cell⁻¹] or, as appropriate, per mass of biological
 446 sample [mol·kg⁻¹]. This approach to specification of dose/exposure provides a scalable
 447 parameter that can be used to design experiments, help interpret a wide variety of experimental
 448 results, and provide absolute information that allows researchers worldwide to make the most
 449 use of published data (Doskey *et al.* 2015).

450 **Phosphorylation, P_», and P_»/O₂ ratio:** *Phosphorylation* in the context of OXPHOS is
 451 defined as phosphorylation of ADP by P_i to form ATP. On the other hand, the term
 452 phosphorylation is used generally in many contexts, *e.g.*, protein phosphorylation. This justifies
 453 consideration of a symbol more discriminating and specific than P as used in the P/O ratio
 454 (phosphate to atomic oxygen ratio), where P indicates phosphorylation of ADP to ATP or GDP
 455 to GTP (**Figure 2**). We propose the symbol P_» for the endergonic (uphill) direction of
 456 phosphorylation ADP→ATP, and likewise the symbol P_« for the corresponding exergonic
 457 (downhill) hydrolysis ATP→ADP (**Figure 3**). P_» refers mainly to electrontransfer
 458 phosphorylation but may also involve substrate-level phosphorylation as part of the
 459 tricarboxylic acid (TCA) cycle (succinyl-CoA ligase; phosphoglycerate kinase) and
 460 phosphorylation of ADP catalyzed by pyruvate kinase, and of GDP phosphorylated by

461 phosphoenolpyruvate carboxykinase. Transphosphorylation is performed by adenylate kinase,
 462 creatine kinase (mtCK), hexokinase and nucleoside diphosphate kinase. In isolated mammalian
 463 mitochondria, ATP production catalyzed by adenylate kinase ($2 \text{ ADP} \leftrightarrow \text{ATP} + \text{AMP}$) proceeds
 464 without fuel substrates in the presence of ADP (Komlódi and Tretter 2017). Kinase cycles are
 465 involved in intracellular energy transfer and signal transduction for regulation of energy flux.
 466

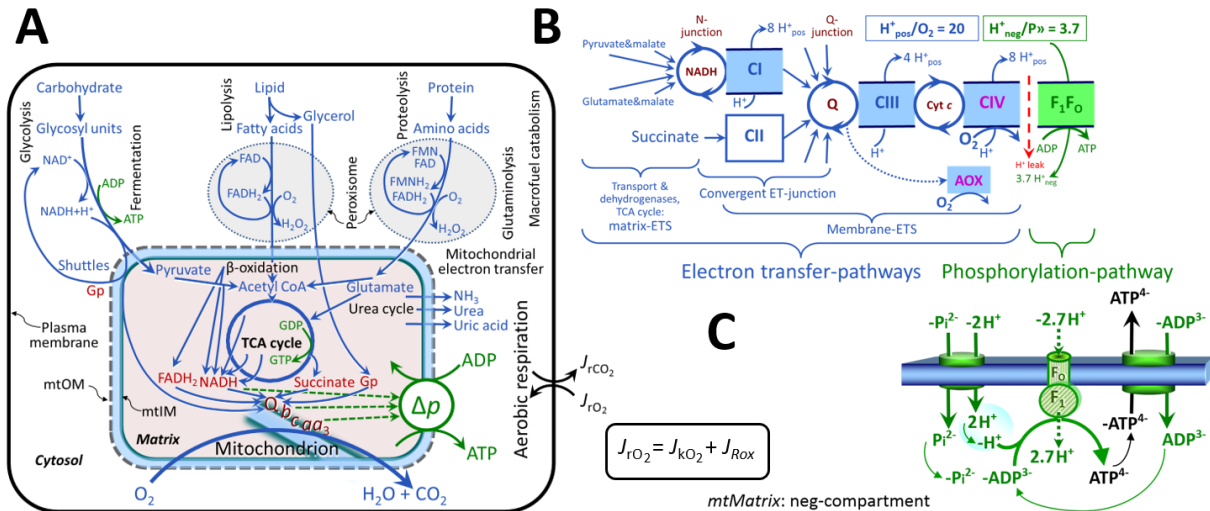


Figure 2. Cell respiration and oxidative phosphorylation (OXPHOS)

467 Mitochondrial respiration is the oxidation of fuel substrates (electron donors) with electron
 468 transfer to O₂ as the electron acceptor. For explanation of symbols see also **Figure 1**.

469 **(A)** Respiration in intact cells: Extra-mitochondrial catabolism of macrofuels or uptake of small
 470 molecules by the cell provides the *mitochondrial* fuel substrates. Many fuel substrates are
 471 catabolized to acetyl-CoA or glutamate, and further electron transfer reduces nicotinamide
 472 adenine dinucleotide to NADH or flavin adenine dinucleotide to FADH₂. In aerobic respiration,
 473 electron transfer is coupled to the phosphorylation of ADP to ATP, with energy transformation
 474 mediated by the protonmotive force, Δp. Anabolic reactions are linked to catabolism, both by
 475 ATP as the intermediary energy currency and by small organic precursor molecules as building
 476 blocks for biosynthesis (not shown). Glycolysis involves substrate-level phosphorylation of
 477 ADP to ATP in fermentation without utilization of O₂. In contrast, extra-mitochondrial
 478 oxidation of fatty acids and amino acids proceeds partially in peroxisomes without coupling to
 479 ATP production: acyl-CoA oxidase catalyzes the oxidation of FADH₂ with electron transfer to
 480 O₂; amino acid oxidases oxidize flavin mononucleotide FMNH₂ or FADH₂. Coenzyme Q, Q,
 481 and the cytochromes *b*, *c*, and *aa*₃ are redox systems of the mitochondrial inner membrane,
 482 mtIM. Dashed arrows indicate the connection between the redox proton pumps (respiratory
 483 Complexes CI, CIII and CIV) and the transmembrane Δp. Mitochondrial outer membrane,
 484 mtOM; glycerol-3-phosphate, Gp; tricarboxylic acid cycle, TCA cycle.

487 **(B)** Respiration in mitochondrial preparations: The mitochondrial electron transfer system
 488 (ETS) is fuelled by diffusion and transport of substrates across the mitochondrial outer and
 489 inner membrane and consists of the matrix-ETS and membrane-ETS. ET-pathways are coupled
 490 to the phosphorylation-pathway. ET-pathways converge at the N-junction and Q-junction.
 491 Additional arrows indicate electron entry into the Q-junction through electron transferring
 492 flavoprotein, glycerophosphate dehydrogenase, dihydro-orotate dehydrogenase, choline
 493 dehydrogenase, and sulfide-ubiquinone oxidoreductase. The dotted arrow indicates the
 494 branched pathway of oxygen consumption by alternative quinol oxidase (AOX). The H⁺_{pos}/O₂
 495 ratio is the outward proton flux from the matrix space to the positively (pos) charged vesicular
 496 compartment, divided by catabolic O₂ flux in the NADH-pathway. The H⁺_{neg}/P ratio is the
 497 inward proton flux from the inter-membrane space to the negatively (neg) charged matrix space,

498 divided by the flux of phosphorylation of ADP to ATP. These are not fixed stoichiometries due
499 to ion leaks and proton slip.

500 (C) Phosphorylation-pathway catalyzed by the proton pump F₁F₀-ATPase (F-ATPase, ATP
501 synthase), adenine nucleotide translocase, and inorganic phosphate transporter. The H⁺_{neg}/P_»
502 stoichiometry is the sum of the coupling stoichiometry in the F-ATPase reaction (-2.7 H⁺_{pos}
503 from the positive intermembrane space, 2.7 H⁺_{neg} to the matrix, *i.e.*, the negative compartment)
504 and the proton balance in the translocation of ADP³⁻, ATP⁴⁻ and P_i²⁻. Modified from (B)
505 Lemieux *et al.* (2017) and (C) Gnaiger (2014).

506

507 The P_»/O₂ ratio (P_»/4 e⁻) is two times the ‘P/O’ ratio (P_»/2 e⁻) of classical bioenergetics.
508 P_»/O₂ is a generalized symbol, not specific for determination of P_i consumption (P_i/O₂ flux
509 ratio), ADP depletion (ADP/O₂ flux ratio), or ATP production (ATP/O₂ flux ratio). The
510 mechanistic P_»/O₂ ratio—or P_»/O₂ stoichiometry—is calculated from the proton-to-O₂ and
511 proton-to-phosphorylation coupling stoichiometries (**Figure 2B**):
512

$$513 \quad P_{\gg}/O_2 = \frac{H_{\text{pos}}^+/O_2}{H_{\text{neg}}^+/P_{\gg}} \quad (1)$$

514

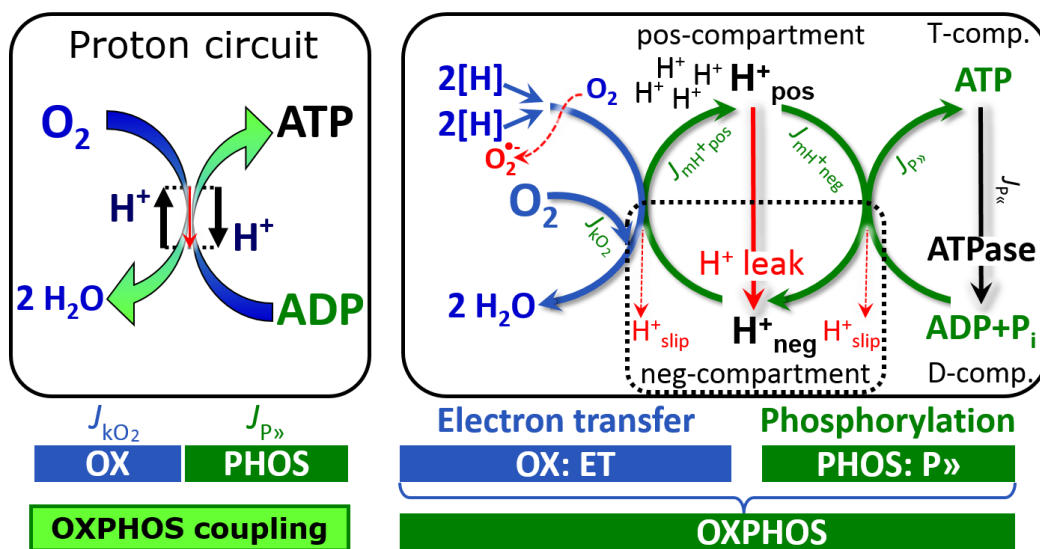
515 The H⁺_{pos}/O₂ *coupling stoichiometry* (referring to the full 4 electron reduction of O₂) depends
516 on the ET-pathway control state, which defines the relative involvement of the three coupling
517 sites (CI, CIII and CIV) in the catabolic pathway of electrons from the oxidation of reduced
518 fuel substrates (electron donors) to the reduction of O₂ (electron acceptor). This varies with: (1)
519 a bypass of CI by single or multiple electron input into the Q-junction; and (2) a bypass of CIV
520 by involvement of alternative oxidases, AOX, which are not expressed in mammalian
521 mitochondria.

522 H⁺_{pos}/O₂ is 12 in the ET-pathways involving CIII and CIV as proton pumps, increasing to
523 20 for the NADH-pathway through CI (**Figure 2B**), but a general consensus on H⁺_{pos}/O₂
524 stoichiometries remains to be reached (Hinkle 2005; Wikström and Hummer 2012; Sazanov
525 2015). The H⁺_{neg}/P_» coupling stoichiometry (3.7; **Figure 2B**) is the sum of 2.7 H⁺_{neg} required
526 by the F-ATPase of vertebrate and most invertebrate species (Watt *et al.* 2010) and the proton
527 balance in the translocation of ADP, ATP and P_i (**Figure 2C**). Taken together, the mechanistic
528 P_»/O₂ ratio is calculated at 5.4 and 3.3 for NADH- and succinate-linked respiration, respectively
529 (Eq. 1). The corresponding classical P_»/O ratios (referring to the 2 electron reduction of 0.5 O₂)
530 are 2.7 and 1.6 (Watt *et al.* 2010), in agreement with the measured P_»/O ratio for succinate of
531 1.58 ± 0.02 (Gnaiger *et al.* 2000).

532 The effective P_»/O₂ flux ratio ($Y_{P_{\gg}/O_2} = J_{P_{\gg}}/J_{kO_2}$; **Figure 3**) is diminished relative to the
533 mechanistic P_»/O₂ ratio by intrinsic and extrinsic uncoupling and dyscoupling (**Figure 4**). Such
534 generalized uncoupling is different from switching to mitochondrial pathways that involve
535 fewer than three proton pumps (‘coupling sites’: Complexes CI, CIII and CIV), bypassing CI
536 through multiple electron entries into the Q-junction, or CIII and CIV through AOX (**Figure**
537 **2B**). Reprogramming of mitochondrial pathways leading to different types of substrates being
538 oxidized may be considered as a switch of gears (changing the stoichiometry by altering the
539 substrate that is oxidized) rather than uncoupling (loosening the tightness of coupling relative
540 to a fixed stoichiometry). In addition, Y_{P_{\gg}/O_2} depends on several experimental conditions of flux
541 control, increasing as a hyperbolic function of [ADP] to a maximum value (Gnaiger 2001).

542 **Control and regulation:** The terms metabolic *control* and *regulation* are frequently used
543 synonymously, but are distinguished in metabolic control analysis: ‘We could understand the
544 regulation as the mechanism that occurs when a system maintains some variable constant over
545 time, in spite of fluctuations in external conditions (homeostasis of the internal state). On the
546 other hand, metabolic control is the power to change the state of the metabolism in response to
547 an external signal’ (Fell 1997). Respiratory control may be induced by experimental control
548 signals that *exert* an influence on: (1) ATP demand and ADP phosphorylation-rate; (2) fuel

549 substrate composition, pathway competition; (3) available amounts of substrates and O_2 , *e.g.*,
 550 starvation and hypoxia; (4) the protonmotive force, redox states, flux–force relationships,
 551 coupling and efficiency; (5) Ca^{2+} and other ions including H^+ ; (6) inhibitors, *e.g.*, nitric oxide
 552 or intermediary metabolites such as oxaloacetate; (7) signalling pathways and regulatory
 553 proteins, *e.g.*, insulin resistance, transcription factor hypoxia inducible factor 1. *Mechanisms* of
 554 respiratory control and regulation include adjustments of: (1) enzyme activities by allosteric
 555 mechanisms and phosphorylation; (2) enzyme content, concentrations of cofactors and
 556 conserved moieties—such as adenylates, nicotinamide adenine dinucleotide [$NAD^+/NADH$],
 557 coenzyme Q, cytochrome *c*; (3) metabolic channeling by supercomplexes; and (4)
 558 mitochondrial density (enzyme concentrations and membrane area) and morphology (cristae
 559 folding, fission and fusion). Mitochondria are targeted directly by hormones, thereby affecting
 560 their energy metabolism (Lee *et al.* 2013; Gerö and Szabo 2016; Price and Dai 2016; Moreno
 561 *et al.* 2017). Evolutionary or acquired differences in the genetic and epigenetic basis of
 562 mitochondrial function (or dysfunction) between individuals; age; gender, biological sex, and
 563 hormone concentrations; life style including exercise and nutrition; and environmental issues
 564 including thermal, atmospheric, toxic and pharmacological factors, exert an influence on all
 565 control mechanisms listed above. For reviews, see Brown 1992; Gnaiger 1993a, 2009; 2014;
 566 Paradies *et al.* 2014; Morrow *et al.* 2017.



568 **Figure 3. Coupling in oxidative phosphorylation (OXPHOS)**
 569 $2[H]$ indicates the reduced hydrogen equivalents of fuel substrates of the catabolic reaction k
 570 with oxygen. O_2 flux, J_{kO_2} , through the catabolic ET-pathway, is coupled to flux through the
 571 phosphorylation-pathway of ADP to ATP, $J_{P\gg}$. The redox proton pumps of the ET-pathway
 572 drive proton flux into the positive (pos) compartment, J_{mH^+pos} , generating the output
 573 protonmotive force (motive, subscript m). F-ATPase is coupled to inward proton current into
 574 the negative (neg) compartment, J_{mH^+neg} , to phosphorylate ADP+ P_i to ATP. The system is
 575 defined by the boundaries (full black line) and is not a black box, but is analysed as a
 576 compartmental system. The negative compartment (neg-compartment, enclosed by the dotted
 577 line) is the matrix space, separated by the mtIM from the positive compartment (pos-
 578 compartment). ADP+ P_i and ATP are the substrate- and product-compartments (scalar ADP and
 579 ATP compartments, D-comp. and T-comp.), respectively. At steady-state proton turnover,
 580 $J_{\infty H^+}$, and ATP turnover, $J_{\infty P}$, maintain concentrations constant, when $J_{mH^+\infty} = J_{mH^+pos} = J_{mH^+neg}$,
 581 and $J_{P\infty} = J_{P\gg} = J_{P\ll}$. Modified from Gnaiger (2014).

582
 583 **Respiratory control and response:** Lack of control by a metabolic pathway, *e.g.*,
 584 phosphorylation-pathway, means that there will be no response to a variable activating it, *e.g.*,

585 [ADP]. The reverse, however, is not true as the absence of a response to [ADP] does not exclude
 586 the phosphorylation-pathway from having some degree of control. The degree of control of a
 587 component of the OXPHOS-pathway on an output variable—such as O₂ flux, will in general
 588 be different from the degree of control on other outputs—such as phosphorylation-flux or
 589 proton leak flux. Therefore, it is necessary to be specific as to which input and output are under
 590 consideration (Fell 1997).

591 **Respiratory coupling control and ET-pathway control:** Respiratory control refers to
 592 the ability of mitochondria to adjust O₂ flux in response to external control signals by engaging
 593 various mechanisms of control and regulation. Respiratory control is monitored in a
 594 mitochondrial preparation under conditions defined as respiratory states. When
 595 phosphorylation of ADP to ATP is stimulated or depressed, an increase or decrease is observed
 596 in electron transfer measured as O₂ flux in respiratory coupling states of intact mitochondria
 597 ('controlled states' in the classical terminology of bioenergetics). Alternatively, coupling of
 598 electron transfer with phosphorylation is disengaged by uncouplers. These protonophores are
 599 weak lipid-soluble acids which disrupt the barrier function of the mtIM and thus shortcircuit
 600 the protonmotive system, functioning like a clutch in a mechanical system. The corresponding
 601 coupling control state is characterized by a high O₂ flux without control by P_o ('uncontrolled
 602 state').

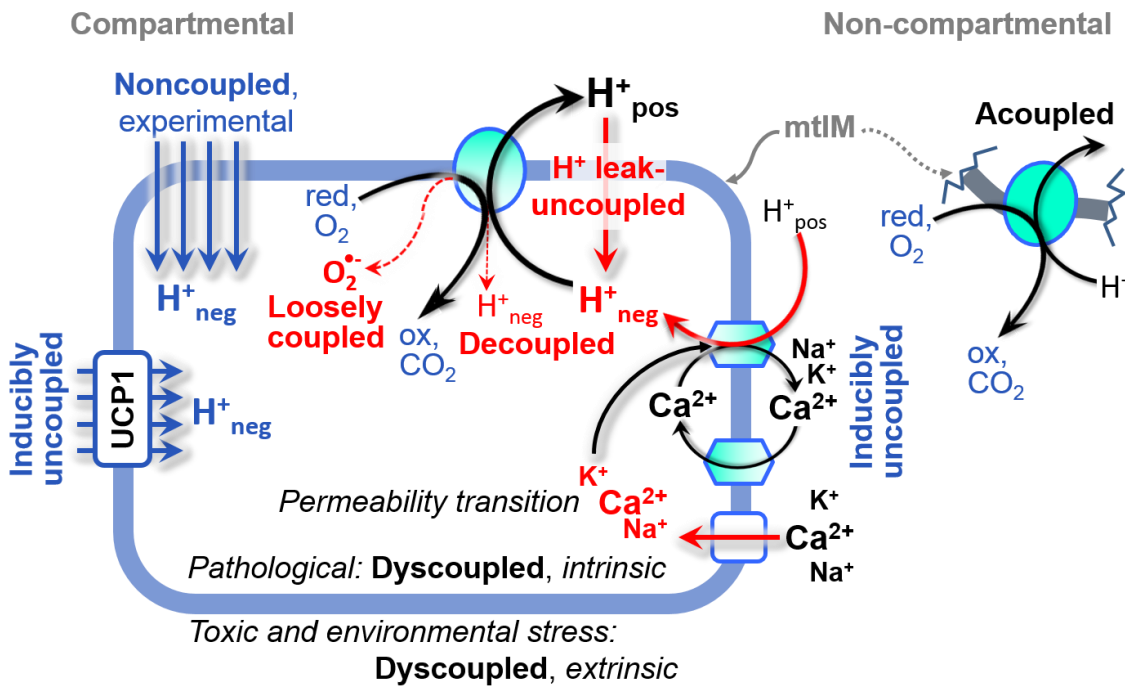
603 ET-pathway control states are obtained in mitochondrial preparations by depletion of
 604 endogenous substrates and addition to the mitochondrial respiration medium of fuel substrates
 605 (2[H] in **Figure 3**) and specific inhibitors, activating selected mitochondrial catabolic pathways,
 606 k, of electron transfer from the oxidation of fuel substrates to reduction of O₂ (**Figure 2A**).
 607 Coupling control states and pathway control states are complementary, since mitochondrial
 608 preparations depend on an exogenous supply of pathway-specific fuel substrates and oxygen
 609 (Gnaiger 2014).

610 **Coupling:** In mitochondrial electron transfer, vectorial transmembrane proton flux is
 611 coupled through the redox proton pumps CI, CIII and CIV to the catabolic flux of scalar
 612 reactions, collectively measured as O₂ flux (**Figure 3**). Thus mitochondria are elements of
 613 energy transformation. Energy is a conserved quantity and cannot be lost or produced in any
 614 internal process (First Law of thermodynamics). Open and closed systems can gain or lose
 615 energy only by external fluxes—by exchange with the environment. Therefore, energy can
 616 neither be produced by mitochondria, nor is there any internal process without energy
 617 conservation. Exergy is defined as the Gibbs energy ('free energy') with the potential to
 618 perform work under conditions of constant volume and pressure. *Coupling* is the interaction of
 619 an exergonic process (spontaneous, negative exergy change) with an endergonic process
 620 (positive exergy change) in energy transformations which conserve part of the exergy that
 621 would be irreversibly lost or dissipated in an uncoupled process.

622 **Uncoupling:** Uncoupling of mitochondrial respiration is a general term comprising
 623 diverse mechanisms:

- 624 1. Proton leak across the mtIM from the pos- to the neg-compartment (**Figure 3**);
- 625 2. Cycling of other cations, strongly stimulated by permeability transition, or
 626 experimentally induced by valinomycin in the presence of K⁺;
- 627 3. Proton slip in the redox proton pumps when protons are effectively not pumped (CI,
 628 CIII and CIV) or are not driving phosphorylation (F-ATPase);
- 629 4. Loss of vesicular (compartmental) integrity when electron transfer is acoupled;
- 630 5. Electron leak in the loosely coupled univalent reduction of O₂ to superoxide (O₂^{•-};
 631 superoxide anion radical).

632 Differences of terms—uncoupled vs. noncoupled—are easily overlooked, although they relate
 633 to different meanings of uncoupling (**Figure 4**).



634
635
636
637
638
639
640
641
642
643
644

Figure 4. Mechanisms of respiratory uncoupling

An intact mitochondrial inner membrane, mtIM, is required for vectorial, compartmental coupling. 'Acoupled' respiration is the consequence of structural disruption with catalytic activity of non-compartmental mitochondrial fragments. Inducibly uncoupled (activation of UCP1) and experimentally noncoupled respiration (titration of protonophores) stimulate respiration to maximum O₂ flux. H⁺ leak-uncoupled, decoupled, and loosely coupled respiration are components of intrinsic uncoupling. Pathological dysfunction may affect all types of uncoupling, including permeability transition, causing intrinsically dyscoupled respiration. Similarly, toxicological and environmental stress factors can cause extrinsically dyscoupled respiration.

645
646
647

2.2. Coupling states and respiratory rates

648
649
650
651
652
653
654
655
656
657

Respiratory capacities in coupling control states: To extend the classical nomenclature on mitochondrial coupling states (Section 2.3) by a concept-driven terminology that explicitly incorporates information on the meaning of respiratory states, the terminology must be general and not restricted to any particular experimental protocol or mitochondrial preparation (Gnaiger 2009). Concept-driven nomenclature aims at mapping the *meaning and concept behind* the words and acronyms onto the *forms* of words and acronyms (Miller 1991). The focus of concept-driven nomenclature is primarily the conceptual 'why', along with clarification of the experimental 'how'. Respiratory capacities delineate, comparable to channel capacity in information theory (Schneider 2006), the upper bound of the rate of respiration measured in defined coupling control states and electron transfer-pathway (ET-pathway) states (Figure 5).

658
659
660
661
662
663
664
665
666

To provide a diagnostic reference for respiratory capacities of core energy metabolism, the capacity of *oxidative phosphorylation*, OXPHOS, is measured at kinetically-saturating concentrations of ADP and P_i. The *oxidative ET-capacity* reveals the limitation of OXPHOS-capacity mediated by the *phosphorylation-pathway*. The ET- and phosphorylation-pathways comprise coupled segments of the OXPHOS-system. ET-capacity is measured as noncoupled respiration by application of *external uncouplers*. The contribution of *intrinsically uncoupled* O₂ consumption is studied by preventing the stimulation of phosphorylation either in the absence of ADP or by inhibition of the phosphorylation-pathway. The corresponding states are collectively classified as LEAK-states, when O₂ consumption compensates mainly for ion

667 leaks, including the proton leak. Defined coupling states are induced by: (1) adding cation
 668 chelators such as EGTA, binding free Ca^{2+} and thus limiting cation cycling; (2) adding ADP
 669 and P_i ; (3) inhibiting the phosphorylation-pathway; and (4) uncoupler titrations, while
 670 maintaining a defined ET-pathway state with constant fuel substrates and inhibitors of specific
 671 branches of the ET-pathway (**Figure 5**).

672

673 **Figure 5. Four-compartment model of oxidative phosphorylation**

674 Respiratory states (ET, OXPHOS, LEAK; **Table 1**) and corresponding rates (E , P , L) are
 675 connected by the protonmotive force, Δp . ET-capacity, E (I), is
 676 partitioned into (2) dissipative LEAK-respiration, L , when the
 677 Gibbs energy change of catabolic

678 O_2 flux is irreversibly lost, (3) net OXPHOS-capacity, $P-L$, with partial conservation of the
 679 capacity to perform work, and (4) the excess capacity, $E-P$. Modified from Gnaiger (2014).

680

681
 682
 683
 684
 685
 686
 687
 688
 689
 690

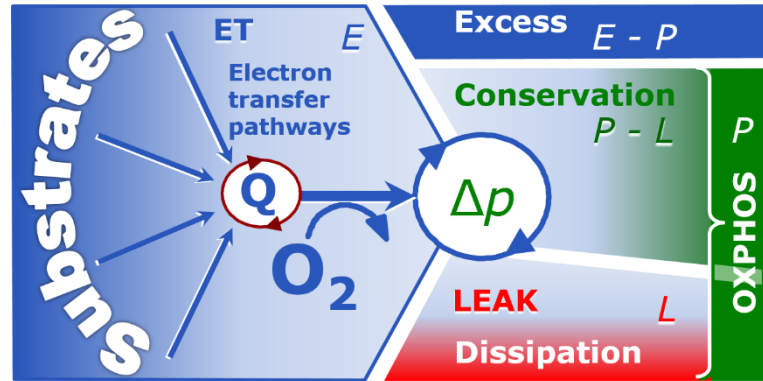


Table 1. Coupling states and residual oxygen consumption in mitochondrial preparations in relation to respiration- and phosphorylation-flux, J_{KO_2} and J_{P} , and protonmotive force, Δp . Coupling states are established at kinetically-saturating concentrations of fuel substrates and O_2 .

State	J_{KO_2}	J_{P}	Δp	Inducing factors	Limiting factors
LEAK	L ; low, cation leak-dependent respiration	0	max.	proton leak, slip, and cation cycling	$J_{\text{P}} = 0$: (1) without ADP, L_N ; (2) max. ATP/ADP ratio, L_T ; or (3) inhibition of the phosphorylation-pathway, L_{Omy}
OXPHOS	P ; high, ADP-stimulated respiration	max.	high	kinetically-saturating [ADP] and [P_i]	J_{P} , by phosphorylation-pathway; or J_{KO_2} by ET-capacity
ET	E ; max., noncoupled respiration	0	low	optimal external uncoupler concentration for max. $J_{\text{O}_2, E}$	J_{KO_2} by ET-capacity
ROX	R_{ox} ; min., residual O_2 consumption	0	0	$J_{\text{O}_2, R_{\text{ox}}}$ in non-ET-pathway oxidation reactions	inhibition of all ET-pathways; or absence of fuel substrates

691

692 The three coupling states, ET, LEAK and OXPHOS, are shown schematically with the
 693 corresponding respiratory rates, abbreviated as E , L and P , respectively (**Figure 5**). We
 694 distinguish metabolic *pathways* from metabolic *states* and the corresponding metabolic *rates*;
 695 for example: ET-pathways (**Figure 5**), ET-states (**Figure 6C**), and ET-capacities, E ,
 696 respectively (**Table 1**). The protonmotive force is *high* in the OXPHOS-state when it drives
 697 phosphorylation, *maximum* in the LEAK-state of coupled mitochondria, driven by LEAK-

698 respiration at a minimum back
 699 flux of cations to the matrix
 700 side, and *very low* in the ET-
 701 state when uncouplers short-
 702 circuit the proton cycle (**Table**
 703 **1**).

704 **LEAK-state** (**Figure**
 705 **6A**): The LEAK-state is defined
 706 as a state of mitochondrial
 707 respiration when O₂ flux mainly
 708 compensates for ion leaks in the
 709 absence of ATP synthesis, at
 710 kinetically-saturating
 711 concentrations of O₂ and
 712 respiratory fuel substrates.
 713 LEAK-respiration is measured
 714 to obtain an estimate of *intrinsic*
 715 *uncoupling* without addition of
 716 an experimental uncoupler: (1)
 717 in the absence of adenylates,
 718 *i.e.*, AMP, ADP and ATP; (2)
 719 after depletion of ADP at a
 720 maximum ATP/ADP ratio; or
 721 (3) after inhibition of the
 722 phosphorylation-pathway by
 723 inhibitors of F-ATPase—such
 724 as oligomycin, or of adenine
 725 nucleotide translocase—such as
 726 carboxyatractyloside.

727 Adjustment of the nominal
 728 concentration of these inhibitors
 729 to the density of biological
 730 sample applied can minimize or
 731 avoid inhibitory side-effects
 732 exerted on ET-capacity or even
 733 some dyscoupling.

734 **Proton leak and**
 735 **uncoupled respiration:** Proton
 736 leak is a leak current of protons.
 737 The intrinsic proton leak is the
 738 *uncoupled* process in which
 739 protons diffuse across the mtIM
 740 in the dissipative direction of the
 741 downhill protonmotive force

742 without coupling to phosphorylation (**Figure 6A**). The proton leak flux depends non-linearly
 743 on the protonmotive force (Garlid *et al.* 1989; Divakaruni and Brand 2011), it is a property of
 744 the mtIM and may be enhanced due to possible contaminations by free fatty acids. Inducible
 745 uncoupling mediated by uncoupling protein 1 (UCP1) is physiologically controlled, *e.g.*, in
 746 brown adipose tissue. UCP1 is a member of the mitochondrial carrier family which is involved
 747 in the translocation of protons across the mtIM (Klingenberg 2017). Consequently, the short-

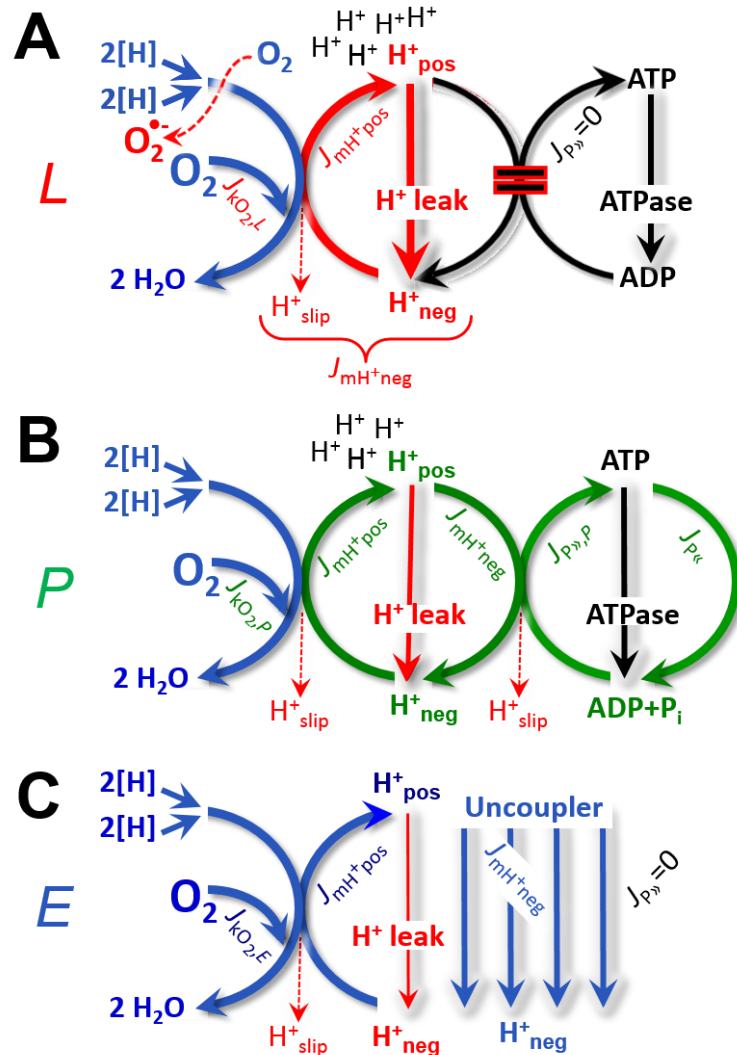


Figure 6. Respiratory coupling states

(A) **LEAK-state and rate, L:** Phosphorylation is arrested, $J_{P_{\gg}} = 0$, and catabolic O₂ flux, $J_{kO_2,L}$, is controlled mainly by the proton leak, $J_{mH^{+}neg,L}$, at maximum protonmotive force (**Figure 4**).

(B) **OXPHOS-state and rate, P:** Phosphorylation, $J_{P_{\gg}}$, is stimulated by kinetically-saturating [ADP] and [P₁], and is supported by a high protonmotive force. O₂ flux, $J_{kO_2,P}$, is well-coupled at a P_{\gg}/O_2 ratio of $J_{P_{\gg},P}/J_{O_2,P}$.

(C) **ET-state and rate, E:** Noncoupled respiration, $J_{kO_2,E}$, is maximum at optimum exogenous uncoupler concentration and phosphorylation is zero, $J_{P_{\gg}} = 0$. See also **Figure 3**.

748 circuit diminishes the protonmotive force and stimulates electron transfer to O₂ and heat
749 dissipation without phosphorylation of ADP.

750 **Cation cycling:** There can be other cation contributors to leak current including calcium
751 and probably magnesium. Calcium influx is balanced by mitochondrial Na⁺/Ca²⁺ or H⁺/Ca²⁺
752 exchange, which is balanced by Na⁺/H⁺ or K⁺/H⁺ exchanges. This is another effective
753 uncoupling mechanism different from proton leak (**Table 2**).

754

755

Table 2. Terms on respiratory coupling and uncoupling.

Term	J_{kO_2}	$P \gg O_2$	Note	
acoupled		0	electron transfer in mitochondrial fragments without vectorial proton translocation (Figure 4)	
intrinsic, no protonophore added	uncoupled	L	0	non-phosphorylating LEAK-respiration (Figure 6A)
	proton leak-uncoupled		0	component of L , H ⁺ diffusion across the mtIM (Figure 4)
	decoupled		0	component of L , proton slip (Figure 4)
	loosely coupled		0	component of L , lower coupling due to superoxide formation and bypass of proton pumps (Figure 4)
	dyscoupled		0	pathologically, toxicologically, environmentally increased uncoupling, mitochondrial dysfunction
	inducibly uncoupled		0	by UCP1 or cation (<i>e.g.</i> , Ca ²⁺) cycling (Figure 4)
noncoupled	E	0	non-phosphorylating respiration stimulated to maximum flux at optimum exogenous uncoupler concentration (Figure 6C)	
well-coupled	P	high	phosphorylating respiration with an intrinsic LEAK component (Figure 6B)	
fully coupled	$P - L$	max.	OXPPOS-capacity corrected for LEAK-respiration (Figure 5)	

756

757

758 **Proton slip and decoupled respiration:** Proton slip is the *decoupled* process in which
759 protons are only partially translocated by a redox proton pump of the ET-pathways and slip
760 back to the original vesicular compartment. The proton leak is the dominant contributor to the
761 overall leak current in mammalian mitochondria incubated under physiological conditions at
762 37 °C, whereas proton slip is increased at lower experimental temperature (Canton *et al.* 1995).
763 Proton slip can also happen in association with the F-ATPase, in which the proton slips downhill
764 across the pump to the matrix without contributing to ATP synthesis. In each case, proton slip
765 is a property of the proton pump and increases with the pump turnover rate.

766

767 **Electron leak and loosely coupled respiration:** Superoxide production by the ETS leads
768 to a bypass of redox proton pumps and correspondingly lower $P \gg O_2$ ratio. This depends on the
769 actual site of electron leak and the scavenging of hydrogen peroxide by cytochrome *c*, whereby
770 electrons may re-enter the ETS with proton translocation by CIV.

771

772 **Loss of compartmental integrity and acoupled respiration:** Electron transfer and
773 catabolic O₂ flux proceed without compartmental proton translocation in disrupted
774 mitochondrial fragments. Such fragments form during mitochondrial isolation, and may not
775 fully fuse to re-establish structurally intact mitochondria. Loss of mtIM integrity, therefore, is

773 the cause of acoupled respiration, which is a nonvectorial dissipative process without control
774 by the protonmotive force.

775 **Dyscoupled respiration:** Mitochondrial injuries may lead to *dyscoupling* as a
776 pathological or toxicological cause of *uncoupled* respiration. Dyscoupling may involve any
777 type of uncoupling mechanism, *e.g.*, opening the permeability transition pore. Dyscoupled
778 respiration is distinguished from the experimentally induced *noncoupled* respiration in the ET-
779 state (**Table 2**).

780 **OXPPOS-state (Figure 6B):** The OXPPOS-state is defined as the respiratory state with
781 kinetically-saturating concentrations of O₂, respiratory and phosphorylation substrates, and
782 absence of exogenous uncoupler, which provides an estimate of the maximal respiratory
783 capacity in the OXPPOS-state for any given ET-pathway state. Respiratory capacities at
784 kinetically-saturating substrate concentrations provide reference values or upper limits of
785 performance, aiming at the generation of data sets for comparative purposes. Physiological
786 activities and effects of substrate kinetics can be evaluated relative to the OXPPOS-capacity.

787 As discussed previously, 0.2 mM ADP does not fully saturate flux in isolated
788 mitochondria (Gnaiger 2001; Puchowicz *et al.* 2004); greater ADP concentration is required,
789 particularly in permeabilized muscle fibres and cardiomyocytes, to overcome limitations by
790 intracellular diffusion and by the reduced conductance of the mtOM (Jepihhina *et al.* 2011,
791 Illaste *et al.* 2012, Simson *et al.* 2016), either through interaction with tubulin (Rostovtseva *et al.*
792 2008) or other intracellular structures (Birkedal *et al.* 2014). In permeabilized muscle fibre
793 bundles of high respiratory capacity, the apparent K_m for ADP increases up to 0.5 mM (Saks *et al.*
794 1998), consistent with experimental evidence that >90% saturation is reached only at >5
795 mM ADP (Pesta and Gnaiger 2012). Similar ADP concentrations are also required for accurate
796 determination of OXPPOS-capacity in human clinical cancer samples and permeabilized cells
797 (Klepinin *et al.* 2016; Koit *et al.* 2017). Whereas 2.5 to 5 mM ADP is sufficient to obtain the
798 actual OXPPOS-capacity in many types of permeabilized tissue and cell preparations,
799 experimental validation is required in each specific case.

800 **Electron transfer-state (Figure 6C):** O₂ flux determined in the ET-state yields an
801 estimate of ET-capacity. The ET-state is defined as the *noncoupled* state with kinetically-
802 saturating concentrations of O₂, respiratory substrate and optimum *exogenous* uncoupler
803 concentration for maximum O₂ flux. As a consequence of the nearly collapsed protonmotive
804 force, the driving force is insufficient for phosphorylation, and $J_{P_s} = 0$. The most frequently
805 used uncouplers are carbonyl cyanide *m*-chloro phenyl hydrazone, carbonyl cyanide *p*-
806 trifluoromethoxyphenylhydrazone or dinitrophenol (CCCP, FCCP, DNP). Stepwise titration
807 of uncouplers stimulates respiration up to or beyond OXPPOS capacity, but inhibition of
808 respiration is observed above optimum uncoupler concentrations. Data obtained with a single
809 dose of uncoupler must be evaluated with caution, particularly when a fixed uncoupler
810 concentration is used in studies exploring a treatment or disease that may alter the mitochondrial
811 content or mitochondrial sensitivity to inhibition by uncouplers.

812 **ROX state and Rox:** Besides the three fundamental coupling states of mitochondrial
813 preparations, the state of residual O₂ consumption, ROX, is relevant to assess respiratory
814 function (**Figure 1**). ROX is not a coupling state. The rate of residual oxygen consumption,
815 *Rox*, is defined as O₂ consumption due to oxidative reactions measured after inhibition of ET—
816 with rotenone, malonic acid and antimycin A. Cyanide and azide inhibit not only CIV but
817 catalase and several peroxidases involved in *Rox*. However, high concentrations of antimycin
818 A, but not rotenone or cyanide, inhibit peroxisomal acyl-CoA oxidase and D-amino acid
819 oxidase (Vamecq *et al.* 1987). ROX represents a baseline that is used to correct respiration
820 measured in defined coupling states. *Rox*-corrected *L*, *P* and *E* not only lower the values of total
821 fluxes, but also changes the flux control ratios *L/P* and *L/E*. *Rox* is not necessarily equivalent
822 to non-mitochondrial reduction of O₂, considering O₂-consuming reactions in mitochondria that
823 are not related to ET—such as O₂ consumption in reactions catalyzed by monoamine oxidases

824 (type A and B), monooxygenases (cytochrome P450 monooxygenases), dioxygenase (sulfur
 825 dioxygenase and trimethyllysine dioxygenase), and several hydroxylases. Even isolated
 826 mitochondrial fractions, especially those obtained from liver, may be contaminated by
 827 peroxisomes. This fact makes the exact determination of mitochondrial O₂ consumption and
 828 mitochondria-associated generation of reactive oxygen species complicated (Schönfeld *et al.*
 829 2009; Spejjer 2016; **Figure 2**). The dependence of ROX-linked O₂ consumption needs to be
 830 studied in detail together with non-ET enzyme activities, availability of specific substrates, O₂
 831 concentration, and electron leakage leading to the formation of reactive oxygen species.

832 **Quantitative relations:** E may exceed or be equal to P . $E > P$ is observed in many types
 833 of mitochondria, varying between species, tissues and cell types (Gnaiger 2009). $E - P$ is the
 834 excess ET-capacity pushing the phosphorylation-flux (**Figure 2C**) to the limit of its *capacity of*
 835 *utilizing* the protonmotive force. In addition, the magnitude of $E - P$ depends on the tightness of
 836 respiratory coupling or degree of uncoupling, since an increase of L causes P to increase
 837 towards the limit of E . The *excess* $E - P$ capacity, $E - P$, therefore, provides a sensitive diagnostic
 838 indicator of specific injuries of the phosphorylation-pathway, under conditions when E remains
 839 constant but P declines relative to controls (**Figure 5**). Substrate cocktails supporting
 840 simultaneous convergent electron transfer to the Q-junction for reconstitution of TCA cycle
 841 function establish pathway control states with high ET-capacity, and consequently increase the
 842 sensitivity of the $E - P$ assay.

843 E cannot theoretically be lower than P . $E < P$ must be discounted as an artefact, which
 844 may be caused experimentally by: (1) loss of oxidative capacity during the time course of the
 845 respirometric assay, since E is measured subsequently to P ; (2) using insufficient uncoupler
 846 concentrations; (3) using high uncoupler concentrations which inhibit ET (Gnaiger 2008); (4)
 847 high oligomycin concentrations applied for measurement of L before titrations of uncoupler,
 848 when oligomycin exerts an inhibitory effect on E . On the other hand, the excess ET-capacity is
 849 overestimated if non-saturating [ADP] or [P_i] are used. See State 3 in the next section.

850 The net OXPHOS-capacity is calculated by subtracting L from P (**Figure 5**). The net
 851 $P \gg O_2$ equals $P \gg (P - L)$, wherein the dissipative LEAK component in the OXPHOS-state may
 852 be overestimated. This can be avoided by measuring LEAK-respiration in a state when the
 853 protonmotive force is adjusted to its slightly lower value in the OXPHOS-state—by titration of
 854 an ET inhibitor (Divakaruni and Brand 2011). Any turnover-dependent components of proton
 855 leak and slip, however, are underestimated under these conditions (Garlid *et al.* 1993). In
 856 general, it is inappropriate to use the term *ATP production* or *ATP turnover* for the difference
 857 of O₂ flux measured in the OXPHOS and LEAK states. $P - L$ is the upper limit of OXPHOS-
 858 capacity that is freely available for ATP production (corrected for LEAK-respiration) and is
 859 fully coupled to phosphorylation with a maximum mechanistic stoichiometry (**Figure 5**).

860 The rates of LEAK respiration and OXPHOS capacity depend on (1) the tightness of
 861 coupling under the influence of the respiratory uncoupling mechanisms (**Figure 4**), and (2) the
 862 coupling stoichiometry which varies as a function of the substrate type undergoing oxidation in
 863 ET-pathways with either two or three coupling sites (**Figure 2B**). When cocktails with NADH-
 864 linked substrates and succinate are used, the relative contribution of ET-pathways with three or
 865 two coupling sites cannot be controlled experimentally, is difficult to determine, and may shift
 866 in transitions between LEAK-, OXPHOS- and ET-states (Gnaiger 2014). Under these
 867 experimental conditions, we cannot separate the tightness of coupling *versus* coupling
 868 stoichiometry as the mechanisms of respiratory control in the shift of L/P ratios. The tightness
 869 of coupling and fully coupled O₂ flux, $P - L$ (**Table 2**), therefore, are obtained from
 870 measurements of coupling control of LEAK respiration, OXPHOS- and ET-capacities in well
 871 defined pathway states, using either pyruvate and malate as substrates or the classical succinate
 872 and rotenone substrate-inhibitor combination (**Figure 2B**).

873
 874

875 2.3. Classical terminology for isolated mitochondria

876 'When a code is familiar enough, it ceases appearing like a code; one forgets that there
877 is a decoding mechanism. The message is identical with its meaning' (Hofstadter 1979).

878

879 Chance and Williams (1955; 1956) introduced five classical states of mitochondrial
880 respiration and cytochrome redox states. **Table 3** shows a protocol with isolated mitochondria
881 in a closed respirometric chamber, defining a sequence of respiratory states. States and rates
882 are not specifically distinguished in this nomenclature.

883

884

885

886

Table 3. Metabolic states of mitochondria (Chance and Williams, 1956; Table V).

State	[O ₂]	ADP level	Substrate level	Respiration rate	Rate-limiting substance
1	>0	low	low	slow	ADP
2	>0	high	~0	slow	substrate
3	>0	high	high	fast	respiratory chain
4	>0	low	high	slow	ADP
5	0	high	high	0	oxygen

887

888 **State 1** is obtained after addition of isolated mitochondria to air-saturated
889 isoosmotic/isotonic respiration medium containing P_i, but no fuel substrates and no adenylates,
890 *i.e.*, AMP, ADP, ATP.

891 **State 2** is induced by addition of a 'high' concentration of ADP (typically 100 to 300
892 μM), which stimulates respiration transiently on the basis of endogenous fuel substrates and
893 phosphorylates only a small portion of the added ADP. State 2 is then obtained at a low
894 respiratory activity limited by exhausted endogenous fuel substrate availability (**Table 3**). If
895 addition of specific inhibitors of respiratory complexes—such as rotenone—does not cause a
896 further decline of O₂ flux, State 2 is equivalent to the ROX state (See below.). If inhibition is
897 observed, undefined endogenous fuel substrates are a confounding factor of pathway control,
898 contributing to the effect of subsequently externally added substrates and inhibitors. In contrast
899 to the original protocol, an alternative sequence of titration steps is frequently applied, in which
900 the alternative 'State 2' has an entirely different meaning, when this second state is induced by
901 addition of fuel substrate without ADP (LEAK-state; in contrast to State 2 defined in **Table 1**
902 as a ROX state), followed by addition of ADP.

903 **State 3** is the state stimulated by addition of fuel substrates while the ADP concentration
904 is still high (**Table 3**) and supports coupled energy transformation through oxidative
905 phosphorylation. 'High ADP' is a concentration of ADP specifically selected to allow the
906 measurement of State 3 to State 4 transitions of isolated mitochondria in a closed respirometric
907 chamber. Repeated ADP titration re-establishes State 3 at 'high ADP'. Starting at O₂
908 concentrations near air-saturation (ca. 200 μM O₂ at sea level and 37 °C), the total ADP
909 concentration added must be low enough (typically 100 to 300 μM) to allow phosphorylation
910 to ATP at a coupled O₂ flux that does not lead to O₂ depletion during the transition to State 4.
911 In contrast, kinetically-saturating ADP concentrations usually are 10-fold higher than 'high
912 ADP', *e.g.*, 2.5 mM in isolated mitochondria. The abbreviation State 3u is occasionally used in
913 bioenergetics, to indicate the state of respiration after titration of an uncoupler, without
914 sufficient emphasis on the fundamental difference between OXPHOS-capacity (*well-coupled*
915 with an *endogenous* uncoupled component) and ET-capacity (*noncoupled*).

916 **State 4** is a LEAK-state that is obtained only if the mitochondrial preparation is intact
917 and well-coupled. Depletion of ADP by phosphorylation to ATP causes a decline of O₂ flux in
918 the transition from State 3 to State 4. Under the conditions of State 4, a maximum protonmotive

919 force and high ATP/ADP ratio are maintained. The gradual decline of Y_{P_{\gg}/O_2} towards
 920 diminishing [ADP] at State 4 must be taken into account for calculation of P_{\gg}/O_2 ratios (Gnaiger
 921 2001). State 4 respiration, L_T (**Table 1**), reflects intrinsic proton leak and ATP hydrolysis
 922 activity. O_2 flux in State 4 is an overestimation of LEAK-respiration if the contaminating ATP
 923 hydrolysis activity recycles some ATP to ADP, $J_{P_{\ll}}$, which stimulates respiration coupled to
 924 phosphorylation, $J_{P_{\gg}} > 0$. This can be tested by inhibition of the phosphorylation-pathway using
 925 oligomycin, ensuring that $J_{P_{\gg}} = 0$ (State 4o). Alternatively, sequential ADP titrations re-
 926 establish State 3, followed by State 3 to State 4 transitions while sufficient O_2 is available.
 927 Anoxia may be reached, however, before exhaustion of ADP (State 5).

928 **State 5** is the state after exhaustion of O_2 in a closed respirometric chamber. Diffusion of
 929 O_2 from the surroundings into the aqueous solution may be a confounding factor preventing
 930 complete anoxia (Gnaiger 2001). Chance and Williams (1955) provide an alternative definition
 931 of State 5, which gives it the different meaning of ROX versus anoxia: ‘State 5 may be obtained
 932 by antimycin A treatment or by anaerobiosis’.

933 In **Table 3**, only States 3 and 4 (and ‘State 2’ in the alternative protocol: addition of fuel
 934 substrates without ADP; not included in the table) are coupling control states, with the
 935 restriction that O_2 flux in State 3 may be limited kinetically by non-saturating ADP
 936 concentrations (**Table 1**).

937
 938

939 3. Normalization: fluxes and flows

940

941 3.1. Normalization: system or sample

942

943 The term *rate* is not sufficiently defined to be useful for reporting data (**Figure 7**). The
 944 inconsistency of the meanings of rate becomes fully apparent when considering Galileo
 945 Galilei’s famous principle, that ‘bodies of different weight all fall at the same rate (have a
 946 constant acceleration)’ (Coopersmith 2010).

947 **Flow per system, I :** In a generalization of electrical terms, flow as an extensive quantity
 948 (I ; per system) is distinguished from flux as a size-specific quantity (J ; per system size) (**Figure**
 949 **7A**). Electric current is flow, I_{el} [$A \equiv C \cdot s^{-1}$] per system (extensive quantity). When dividing this
 950 extensive quantity by system size (cross-sectional area of a ‘wire’), a size-specific quantity is
 951 obtained, which is flux (current density), J_{el} [$A \cdot m^{-2} = C \cdot s^{-1} \cdot m^{-2}$] (**Box 2**).

952

953 **Box 2: Metabolic fluxes and flows: vectorial and scalar**

954

955 Fluxes are *vectors*, if they have *spatial* geometric direction in addition to magnitude.
 956 Electric charge per unit time is electric flow or current, $I_{el} = dQ_{el} \cdot dt^{-1}$ [A]. When expressed per
 957 unit cross-sectional area, A [m^2], a vector flux is obtained, which is current density (surface-
 958 density of flow) perpendicular to the direction of flux, $J_{el} = I_{el} \cdot A^{-1}$ [$A \cdot m^{-2}$] (Cohen et al. 2008).
 959 For all transformations *flows*, I_{tr} , are defined as extensive quantities. Vector and scalar *fluxes*
 960 are obtained as $J_{tr} = I_{tr} \cdot A^{-1}$ [$mol \cdot s^{-1} \cdot m^{-2}$] and $J_{tr} = I_{tr} \cdot V^{-1}$ [$mol \cdot s^{-1} \cdot m^{-3}$], expressing flux as an area-
 961 specific vector or volume-specific vectorial or scalar quantity, respectively (Gnaiger 1993b).
 962 We use the metre–kilogram–second–ampere (MKSA) international system of units (*SI*) for
 963 general cases ([m], [kg], [s] and [A]), with decimal *SI* prefixes for specific applications (**Table**
 964 **4**).

965 We suggest to define: (1) *vectorial* fluxes, which are translocations as functions of
 966 *gradients* with direction in geometric space in continuous systems; (2) *vectorial* fluxes, which
 967 describe translocations in discontinuous systems and are restricted to information on
 968 *compartmental differences* (**Figure 3**, transmembrane proton flux); and (3) *scalar* fluxes, which
 969 are transformations in a *homogenous* system (**Figure 3**, catabolic O_2 flux, J_{kO_2}).

970 Vectorial transmembrane proton fluxes, $J_{mH^{+}pos}$ and $J_{mH^{+}neg}$, are analyzed in a
 971 heterogenous compartmental system as a quantity with *directional* but not *spatial* information.
 972 Translocation of protons across the mtIM has a defined direction, either from the negative
 973 compartment (matrix space; negative, neg–compartment) to the positive compartment (inter-
 974 membrane space; positive, pos–compartment) or *vice versa* (**Figure 3**). The arrows defining
 975 the direction of the translocation between the two vesicular compartments may point upwards
 976 or downwards, right or left, without any implication that these are actual directions in space.
 977 The pos–compartment is neither above nor below the neg–compartment in a spatial sense, but
 978 can be visualized arbitrarily in a figure in the upper position (**Figure 3**). In general, the
 979 *compartmental direction* of vectorial translocation from the neg–compartment to the pos–
 980 compartment is defined by assigning the initial and final state as *ergodynamic compartments*,
 981 $H^{+}_{neg} \rightarrow H^{+}_{pos}$ or $0 = -1 H^{+}_{neg} + 1 H^{+}_{pos}$, related to work (erg = work) that must be performed to
 982 lift the proton from a lower to a higher electrochemical potential or from the lower to the higher
 983 ergodynamic compartment (Gnaiger 1993b).

984 In analogy to *vectorial* translocation, the direction of a *scalar* chemical reaction, $A \rightarrow B$
 985 or $0 = -1 A + 1 B$, is defined by assigning substrates and products, A and B, as ergodynamic
 986 compartments. O_2 is defined as a substrate in respiratory O_2 consumption (electron acceptor),
 987 which together with the fuel substrates (electron donors) comprises the substrate compartment
 988 of the catabolic reaction. Volume-specific scalar O_2 flux is coupled to vectorial translocation,
 989 yielding the H^{+}_{pos}/O_2 ratio (**Figure 2B**).

990
 991 **Extensive quantities:** An extensive quantity increases proportionally with system size.
 992 The magnitude of an extensive quantity is completely additive for non-interacting
 993 subsystems—such as mass or flow expressed per defined system. The magnitude of these
 994 quantities depends on the extent or size of the system (Cohen *et al.* 2008).

995 **Size-specific quantities:** ‘The adjective *specific* before the name of an extensive quantity
 996 is often used to mean *divided by mass*’ (Cohen *et al.* 2008). In this system-paradigm, mass-
 997 specific flux is flow divided by mass of the *system* (the total mass of everything within the
 998 measuring chamber or reactor). A mass-specific quantity is independent of the extent of non-
 999 interacting homogenous subsystems. Tissue-specific quantities (related to the *sample* in
 1000 contrast to the *system*) are of fundamental interest in the field of comparative mitochondrial
 1001 physiology, where *specific* refers to the *type of the sample* rather than *mass of the system*. The
 1002 term *specific*, therefore, must be clarified; *sample-specific*, e.g., muscle mass-specific
 1003 normalization, is distinguished from *system-specific* quantities (mass or volume; **Figure 7**).

1004 3.2. Normalization for system-size: flux per chamber volume

1005
 1006
 1007 **System-specific flux, J_{V,O_2} :** The experimental system (experimental chamber) is part of
 1008 the measurement apparatus, separated from the environment as an isolated, closed, open,
 1009 isothermal or non-isothermal system (**Table 4**). On another level, we distinguish between (1)
 1010 the *system* with volume V and mass m defined by the system boundaries, and (2) the *sample* or
 1011 *objects* with volume V_X and mass m_X that are enclosed in the experimental chamber (**Figure 7**).
 1012 Metabolic O_2 flow per object, $I_{O_2/X}$, increases as the mass of the object is increased. Sample
 1013 mass-specific O_2 flux, $J_{O_2/mX}$ should be independent of the mass of the sample studied in the
 1014 instrument chamber, but system volume-specific O_2 flux, J_{V,O_2} (per volume of the instrument
 1015 chamber), should increase in direct proportion to the mass of the sample in the chamber.
 1016 Whereas J_{V,O_2} depends on mass-concentration of the sample in the chamber, it should be
 1017 independent of the chamber (system) volume at constant sample mass. There are practical
 1018 limitations to increase the mass-concentration of the sample in the chamber, when one is
 1019 concerned about crowding effects and instrumental time resolution.

1020 **Figure 7. Flow and flux, and**
 1021 **normalization in structure-**
 1022 **function analysis**

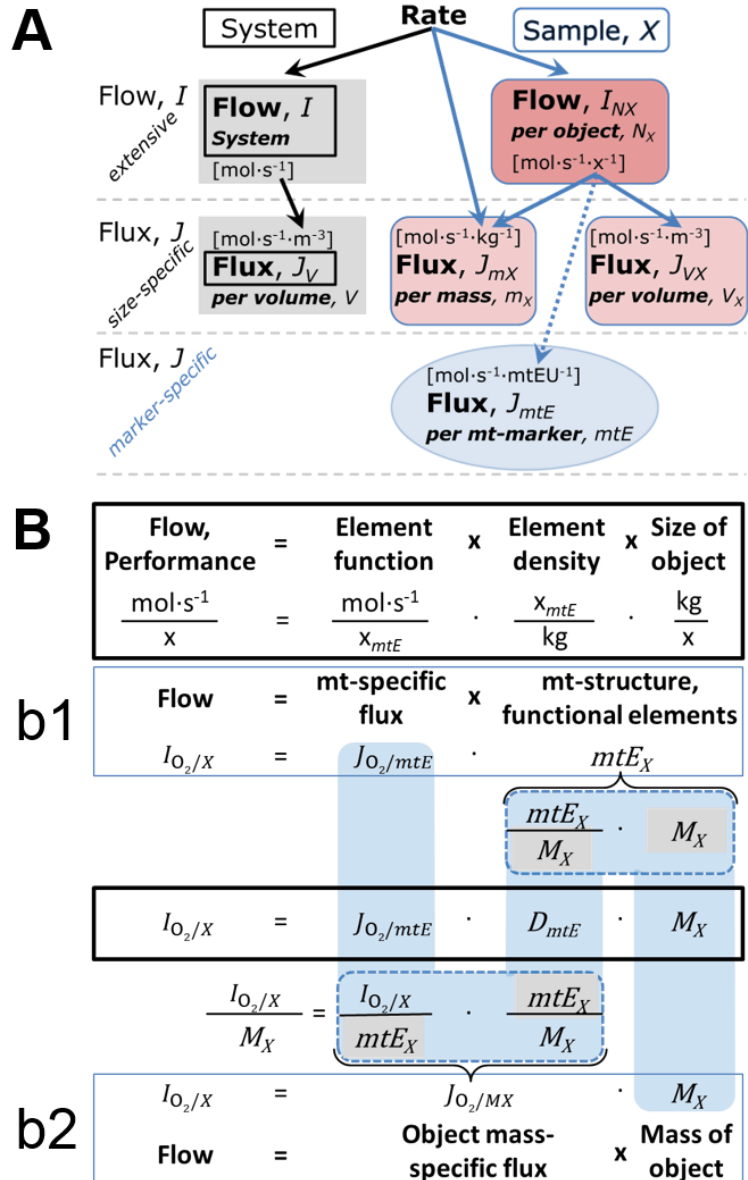
1023 (A) Different meanings of rate
 1024 may lead to confusion, if the
 1025 normalization is not sufficiently
 1026 specified. Results are frequently
 1027 expressed as mass-specific *flux*,
 1028 J_{mX} , per mg protein, dry or wet
 1029 weight (mass). Cell volume, V_{cell} ,
 1030 may be used for normalization
 1031 (volume-specific flux, $J_{V\text{cell}}$),
 1032 which must be clearly
 1033 distinguished from flow per cell,
 1034 $I_{N\text{cell}}$, or flux, J_V , expressed for
 1035 methodological reasons per
 1036 volume of the measurement
 1037 system.

1038 (B) O_2 flow, $I_{O_2/X}$, is the product
 1039 of performance per functional
 1040 element (element function,
 1041 mitochondria-specific flux),
 1042 element density (mitochondrial
 1043 density, D_{mtE}), and size of entity X
 1044 (mass, M_X). (b1) Structured
 1045 analysis: performance is the
 1046 product of mitochondrial *function*
 1047 (mt-specific flux) and *structure*
 1048 (functional elements; D_{mtE} times
 1049 mass of X). (b2) Unstructured
 1050 analysis: performance is the
 1051 product of *entity mass-specific*
 1052 flux, $J_{O_2/MX} = I_{O_2/X}/M_X = I_{O_2}/m_X$

1053 $[\text{mol}\cdot\text{s}^{-1}\cdot\text{kg}^{-1}]$ and *size of entity*, expressed as mass of X ; $M_X = m_X\cdot N_X^{-1} [\text{kg}\cdot\text{x}^{-1}]$. Modified from
 1054 Gnaiger (2014). For further details see **Table 4**.

1055

1056 When the reactor volume does not change during the reaction, which is typical for liquid
 1057 phase reactions, the volume-specific *flux of a chemical reaction* r is the time derivative of the
 1058 advancement of the reaction per unit volume, $J_{V,rB} = d_{r\zeta_B}/dt\cdot V^{-1} [(\text{mol}\cdot\text{s}^{-1})\cdot\text{L}^{-1}]$. The *rate of*
 1059 *concentration change* is $dc_B/dt [(\text{mol}\cdot\text{L}^{-1})\cdot\text{s}^{-1}]$, where concentration is $c_B = n_B/V$. There is a
 1060 difference between (1) $J_{V,rO_2} [\text{mol}\cdot\text{s}^{-1}\cdot\text{L}^{-1}]$ and (2) rate of concentration change $[\text{mol}\cdot\text{L}^{-1}\cdot\text{s}^{-1}]$.
 1061 These merge to a single expression only in closed systems. In open systems, external fluxes
 1062 (such as O_2 supply) are distinguished from internal transformations (catabolic flux, O_2
 1063 consumption). In a closed system, external flows of all substances are zero and O_2 consumption
 1064 (internal flow of catabolic reactions k), $I_{kO_2} [\text{pmol}\cdot\text{s}^{-1}]$, causes a decline of the amount of O_2
 1065 in the system, $n_{O_2} [\text{nmol}]$. Normalization of these quantities for the volume of the system, $V [\text{L} \equiv$
 1066 $\text{dm}^3]$, yields volume-specific O_2 flux, $J_{V,kO_2} = I_{kO_2}/V [\text{nmol}\cdot\text{s}^{-1}\cdot\text{L}^{-1}]$, and O_2 concentration, $[O_2]$
 1067 or $c_{O_2} = n_{O_2}/V [\mu\text{mol}\cdot\text{L}^{-1} = \mu\text{M} = \text{nmol}\cdot\text{mL}^{-1}]$. Instrumental background O_2 flux is due to external
 1068 flux into a non-ideal closed respirometer; then total volume-specific flux has to be corrected for
 1069 instrumental background O_2 flux— O_2 diffusion into or out of the instrumental chamber. J_{V,kO_2}
 1070 is relevant mainly for methodological reasons and should be compared with the accuracy of



1071 instrumental resolution of background-corrected flux, *e.g.*, $\pm 1 \text{ nmol}\cdot\text{s}^{-1}\cdot\text{L}^{-1}$ (Gnaiger 2001).
 1072 ‘Metabolic’ or catabolic indicates O_2 flux, J_{kO_2} , corrected for: (1) instrumental background O_2
 1073 flux; (2) chemical background O_2 flux due to autoxidation of chemical components added to
 1074 the incubation medium; and (3) R_{ox} for O_2 -consuming side reactions unrelated to the catabolic
 1075 pathway k.

1077 3.3. Normalization: per sample

1078
 1079 The challenges of measuring mitochondrial respiratory flux are matched by those of
 1080 normalization. Application of common and defined units is required for direct transfer of
 1081 reported results into a database. The second [s] is the *SI* unit for the base quantity *time*. It is also
 1082 the standard time-unit used in solution chemical kinetics. A rate may be considered as the
 1083 numerator and normalization as the complementary denominator, which are tightly linked in
 1084 reporting the measurements in a format commensurate with the requirements of a database.
 1085 Normalization (Table 4) is guided by physicochemical principles, methodological
 1086 considerations, and conceptual strategies (Figure 7).

1087 **Sample concentration, C_{mX} :** Normalization for sample concentration is required to
 1088 report respiratory data. Considering a tissue or cells as the sample, X, the sample mass is m_X
 1089 [mg], which is frequently measured as wet or dry weight, W_w or W_d [mg], respectively, or as
 1090 amount of tissue or cell protein, m_{Protein} . In the case of permeabilized tissues, cells, and
 1091 homogenates, the sample concentration, $C_{mX} = m_X/V$ [$\text{g}\cdot\text{L}^{-1} = \text{mg}\cdot\text{mL}^{-1}$], is the mass of the
 1092 subsample of tissue that is transferred into the instrument chamber.

1093 **Mass-specific flux, $J_{\text{O}_2/mX}$:** Mass-specific flux is obtained by expressing respiration per
 1094 mass of sample, m_X [mg]. X is the type of sample—isolated mitochondria, tissue homogenate,
 1095 permeabilized fibres or cells. Volume-specific flux is divided by mass concentration of X, $J_{\text{O}_2/mX}$
 1096 $= J_{V,\text{O}_2}/C_{mX}$; or flow per cell is divided by mass per cell, $J_{\text{O}_2/m\text{cell}} = I_{\text{O}_2/\text{cell}}/M_{\text{cell}}$. If mass-specific
 1097 O_2 flux is constant and independent of sample size (expressed as mass), then there is no
 1098 interaction between the subsystems. A 1.5 mg and a 3.0 mg muscle sample respire at identical
 1099 mass-specific flux. Mass-specific O_2 flux, however, may change with the mass of a tissue
 1100 sample, cells or isolated mitochondria in the measuring chamber, in which the nature of the
 1101 interaction becomes an issue. Therefore, cell density must be optimized, particularly in
 1102 experiments carried out in wells, considering the confluency of the cell monolayer or clumps
 1103 of cells (Salabei *et al.* 2014).

1104 **Number concentration, C_{NX} :** C_{NX} is the experimental *number concentration* of sample
 1105 X. In the case of cells or animals, *e.g.*, nematodes, $C_{NX} = N_X/V$ [$\text{x}\cdot\text{L}^{-1}$], where N_X is the number
 1106 of cells or organisms in the chamber (Table 4).

1107 **Flow per object, $I_{\text{O}_2/X}$:** A special case of normalization is encountered in respiratory
 1108 studies with permeabilized (or intact) cells. If respiration is expressed per cell, the O_2 flow per
 1109 measurement system is replaced by the O_2 flow per cell, $I_{\text{O}_2/\text{cell}}$ (Table 4). O_2 flow can be
 1110 calculated from volume-specific O_2 flux, J_{V,O_2} [$\text{nmol}\cdot\text{s}^{-1}\cdot\text{L}^{-1}$] (per V of the measurement chamber
 1111 [L]), divided by the number concentration of cells, $C_{N\text{cell}} = N_{\text{cell}}/V$ [$\text{cell}\cdot\text{L}^{-1}$], where N_{cell} is the
 1112 number of cells in the chamber. The total cell count is the sum of viable and dead cells, $N_{\text{cell}} =$
 1113 $N_{\text{vce}} + N_{\text{dce}}$ (Table 5). The cell viability index, $\text{CVI} = N_{\text{vce}}/N_{\text{cell}}$, is the ratio of viable cells (N_{vce} ;
 1114 before experimental permeabilization) per total cell count. After experimental permeabilization,
 1115 all cells are permeabilized, $N_{\text{pce}} = N_{\text{cell}}$. The cell viability index can be used to normalize
 1116 respiration for the number of cells that have been viable before experimental permeabilization,
 1117 $I_{\text{O}_2/\text{vce}} = I_{\text{O}_2/\text{cell}}/\text{CVI}$, considering that mitochondrial respiratory dysfunction in dead cells should
 1118 be eliminated as a confounding factor.

1119 Cellular O_2 flow can be compared between cells of identical size. To take into account
 1120 changes and differences in cell size, normalization is required to obtain cell size-specific or
 1121 mitochondrial marker-specific O_2 flux (Renner *et al.* 2003).

Table 4. Sample concentrations and normalization of flux.

Expression	Symbol	Definition	Unit	Notes
Sample				
identity of sample	X	object: cell, tissue, animal, patient		
number of sample entities X	N_X	number of objects	x	
mass of sample X	m_X		kg	1
mass of object X	M_X	$M_X = m_X \cdot N_X^{-1}$	$\text{kg} \cdot \text{x}^{-1}$	1
Mitochondria				
mitochondria	mt	$X = \text{mt}$		
amount of mt-elements	mtE	quantity of mt-marker	mtEU	
Concentrations				
object number concentration	C_{NX}	$C_{NX} = N_X \cdot V^{-1}$	$\text{x} \cdot \text{m}^{-3}$	2
sample mass concentration	C_{mX}	$C_{mX} = m_X \cdot V^{-1}$	$\text{kg} \cdot \text{m}^{-3}$	
mitochondrial concentration	C_{mtE}	$C_{mtE} = mtE \cdot V^{-1}$	$\text{mtEU} \cdot \text{m}^{-3}$	3
specific mitochondrial density	D_{mtE}	$D_{mtE} = mtE \cdot m_X^{-1}$	$\text{mtEU} \cdot \text{kg}^{-1}$	4
mitochondrial content, mtE per object X	mtE_X	$mtE_X = mtE \cdot N_X^{-1}$	$\text{mtEU} \cdot \text{x}^{-1}$	5
O₂ flow and flux				
flow, system	I_{O_2}	internal flow	$\text{mol} \cdot \text{s}^{-1}$	6
volume-specific flux	J_{V,O_2}	$J_{V,O_2} = I_{O_2} \cdot V^{-1}$	$\text{mol} \cdot \text{s}^{-1} \cdot \text{m}^{-3}$	7
flow per object X	$I_{O_2/X}$	$I_{O_2/X} = J_{V,O_2} \cdot C_{NX}^{-1}$	$\text{mol} \cdot \text{s}^{-1} \cdot \text{x}^{-1}$	8
mass-specific flux	$J_{O_2/mX}$	$J_{O_2/mX} = J_{V,O_2} \cdot C_{mX}^{-1}$	$\text{mol} \cdot \text{s}^{-1} \cdot \text{kg}^{-1}$	9
mitochondria-specific flux	$J_{O_2/mtE}$	$J_{O_2/mtE} = J_{V,O_2} \cdot C_{mtE}^{-1}$	$\text{mol} \cdot \text{s}^{-1} \cdot \text{mtEU}^{-1}$	10

- 1124 1 Units are given in the MKSA system (**Box 2**). The *SI* prefix k is used for the *SI* base unit of mass (kg
1125 = 1,000 g). In praxis, various *SI* prefixes are used for convenience, to make numbers easily readable,
1126 e.g., 1 mg tissue, cell or mitochondrial mass instead of 0.000001 kg.
- 1127 2 In case sample $X = \text{cells}$, the object number concentration is $C_{N_{\text{cell}}} = N_{\text{cell}} \cdot V^{-1}$, and volume may be
1128 expressed in [$\text{dm}^3 \equiv \text{L}$] or [$\text{cm}^3 = \text{mL}$]. See **Table 5** for different object types.
- 1129 3 mt-concentration is an experimental variable, dependent on sample concentration: (1) $C_{mtE} = mtE \cdot V^{-1}$;
1130 (2) $C_{mtE} = mtE_X \cdot C_{NX}$; (3) $C_{mtE} = C_{mX} \cdot D_{mtE}$.
- 1131 4 If the amount of mitochondria, mtE , is expressed as mitochondrial mass, then D_{mtE} is the mass
1132 fraction of mitochondria in the sample. If mtE is expressed as mitochondrial volume, V_{mt} , and the
1133 mass of sample, m_X , is replaced by volume of sample, V_X , then D_{mtE} is the volume fraction of
1134 mitochondria in the sample.
- 1135 5 $mtE_X = mtE \cdot N_X^{-1} = C_{mtE} \cdot C_{NX}^{-1}$.
- 1136 6 O₂ can be replaced by other chemicals B to study different reactions, e.g., ATP, H₂O₂, or vesicular
1137 compartmental translocations, e.g., Ca²⁺.
- 1138 7 I_{O_2} and V are defined per instrument chamber as a system of constant volume (and constant
1139 temperature), which may be closed or open. I_{O_2} is abbreviated for I_{r,O_2} , i.e., the metabolic or internal
1140 O₂ flow of the chemical reaction r in which O₂ is consumed, hence the negative stoichiometric
1141 number, $\nu_{O_2} = -1$. $I_{r,O_2} = d_r n_{O_2} / dt \cdot \nu_{O_2}^{-1}$. If r includes all chemical reactions in which O₂ participates, then
1142 $d_r n_{O_2} = dn_{O_2} - d_e n_{O_2}$, where dn_{O_2} is the change in the amount of O₂ in the instrument chamber and $d_e n_{O_2}$
1143 is the amount of O₂ added externally to the system. At steady state, by definition $dn_{O_2} = 0$, hence $d_r n_{O_2}$
1144 $= -d_e n_{O_2}$.
- 1145 8 J_{V,O_2} is an experimental variable, expressed per volume of the instrument chamber.
- 1146 9 $I_{O_2/X}$ is a physiological variable, depending on the size of entity X .
- 1147 10 There are many ways to normalize for a mitochondrial marker, that are used in different experimental
1148 approaches: (1) $J_{O_2/mtE} = J_{V,O_2} \cdot C_{mtE}^{-1}$; (2) $J_{O_2/mtE} = J_{V,O_2} \cdot C_{mX}^{-1} \cdot D_{mtE}^{-1} = J_{O_2/mX} \cdot D_{mtE}^{-1}$; (3) $J_{O_2/mtE} =$
1149 $J_{V,O_2} \cdot C_{NX}^{-1} \cdot mtE_X^{-1} = I_{O_2/X} \cdot mtE_X^{-1}$; (4) $J_{O_2/mtE} = I_{O_2} \cdot mtE^{-1}$. The mt-elemental unit [mtEU] varies between
1150 different mt-markers.

1151

Table 5. Sample types, X, abbreviations, and quantification.

Identity of sample	X	N_X	Mass ^a	Volume	mt-Marker
mitochondrial preparation	mt-prep	[x]	[kg]	[m ³]	[mtEU]
isolated mitochondria	imt		m_{mt}	V_{mt}	mtE
tissue homogenate	thom		m_{thom}		mtE_{thom}
permeabilized tissue	pti		m_{pti}		mtE_{pti}
permeabilized fibre	pfi		m_{pfi}		mtE_{pfi}
permeabilized cell	pce	N_{pce}	M_{pce}	V_{pce}	mtE_{pce}
cells ^b	cell	N_{cell}	M_{cell}	V_{cell}	mtE_{cell}
intact cell, viable cell	vce	N_{vce}	M_{vce}	V_{vce}	
dead cell	dce	N_{dce}	M_{dce}	V_{dce}	
organism	org	N_{org}	M_{org}	V_{org}	

1152

^a Instead of mass, the wet weight or dry weight is frequently stated, W_w or W_d .

1153

m_X is mass of the sample [kg], M_X is mass of the object [$kg \cdot x^{-1}$].

1154

^b Total cell count, $N_{cell} = N_{vce} + N_{dce}$

1155

1156

1157

1158

1159

1160

1161

1162

1163

1164

1165

3.4. Normalization for mitochondrial content

1166

1167

1168

1169

1170

1171

1172

1173

1174

1175

Tissues can contain multiple cell populations that may have distinct mitochondrial subtypes. Mitochondria undergo dynamic fission and fusion cycles, and can exist in multiple stages and sizes that may be altered by a range of factors. The isolation of mitochondria (often achieved through differential centrifugation) can therefore yield a subsample of the mitochondrial types present in a tissue, depending on the isolation protocols utilized (*e.g.*, centrifugation speed). This possible bias should be taken into account when planning experiments using isolated mitochondria. Different sizes of mitochondria are enriched at specific centrifugation speeds, which can be used strategically for isolation of mitochondrial subpopulations.

1176

1177

1178

1179

1180

1181

1182

1183

Part of the mitochondrial content of a tissue is lost during preparation of isolated mitochondria. The fraction of isolated mitochondria obtained from a tissue sample is expressed as mitochondrial recovery. At a high mitochondrial recovery the fraction of isolated mitochondria is more representative of the total mitochondrial population than in preparations characterized by low recovery. Determination of the mitochondrial recovery and yield is based on measurement of the concentration of a mitochondrial marker in the stock of isolated mitochondria, $C_{mtE,stock}$, and crude tissue homogenate, $C_{mtE,thom}$, which simultaneously provides information on the specific mitochondrial density in the sample, D_{mtE} (Table 4).

1184

1185

1186

1187

1188

Normalization is a problematic subject; it is essential to consider the question of the study. If the study aims at comparing tissue performance—such as the effects of a treatment on a specific tissue, then normalization for tissue mass or protein content is appropriate. However, if the aim is to find differences on mitochondrial function independent of mitochondrial density (Table 4), then normalization to a mitochondrial marker is imperative (Figure 7). One cannot

1189 assume that quantitative changes in various markers—such as mitochondrial proteins—
 1190 necessarily occur in parallel with one another. It should be established that the marker chosen
 1191 is not selectively altered by the performed treatment. In conclusion, the normalization must
 1192 reflect the question under investigation to reach a satisfying answer. On the other hand, the goal
 1193 of comparing results across projects and institutions requires standardization on normalization
 1194 for entry into a databank.

1195 **Mitochondrial concentration, C_{mtE} , and mitochondrial markers:** Mitochondrial
 1196 organelles comprise a dynamic cellular reticulum in various states of fusion and fission. Hence,
 1197 the definition of an "amount" of mitochondria is often misconceived: mitochondria cannot be
 1198 counted reliably as a number of occurring elements. Therefore, quantification of the "amount"
 1199 of mitochondria depends on the measurement of chosen mitochondrial markers. 'Mitochondria
 1200 are the structural and functional elemental units of cell respiration' (Gnaiger 2014). The
 1201 quantity of a mitochondrial marker can reflect the amount of *mitochondrial elements, mtE*,
 1202 expressed in various mitochondrial elemental units [mtEU] specific for each measured mt-
 1203 marker (**Table 4**). However, since mitochondrial quality may change in response to stimuli—
 1204 particularly in mitochondrial dysfunction (Campos *et al.* 2017) and after exercise training (Pesta
 1205 *et al.* 2011) and during aging (Daum *et al.* 2013)—some markers can vary while others are
 1206 unchanged: (1) Mitochondrial volume and membrane area are structural markers, whereas
 1207 mitochondrial protein mass is frequently used as a marker for isolated mitochondria. (2)
 1208 Molecular and enzymatic mitochondrial markers (amounts or activities) can be selected as
 1209 matrix markers, *e.g.*, citrate synthase activity, mtDNA; mtIM-markers, *e.g.*, cytochrome *c*
 1210 oxidase activity, *aa₃* content, cardiolipin, or mtOM-markers, *e.g.*, the voltage-dependent anion
 1211 channel (VDAC), TOM20. (3) Extending the measurement of mitochondrial marker enzyme
 1212 activity to mitochondrial pathway capacity, ET- or OXPHOS-capacity can be considered as an
 1213 integrative functional mitochondrial marker.

1214 Depending on the type of mitochondrial marker, the mitochondrial elements, *mtE*, are
 1215 expressed in marker-specific units. Mitochondrial concentration in the measurement chamber
 1216 and the tissue of origin are quantified as (1) a quantity for normalization in functional analyses,
 1217 C_{mtE} , and (2) a physiological output that is the result of mitochondrial biogenesis and
 1218 degradation, D_{mtE} , respectively (**Table 4**). It is recommended, therefore, to distinguish
 1219 *experimental mitochondrial concentration*, $C_{mtE} = mtE/V$ and *physiological mitochondrial*
 1220 *density*, $D_{mtE} = mtE/m_X$. Then mitochondrial density is the amount of mitochondrial elements
 1221 per mass of tissue, which is a biological variable (**Figure 7**). The experimental variable is
 1222 mitochondrial density multiplied by sample mass concentration in the measuring chamber, C_{mtE}
 1223 $= D_{mtE} \cdot C_{mX}$, or mitochondrial content multiplied by sample number concentration, $C_{mtE} =$
 1224 $mtE_X \cdot C_{NX}$ (**Table 4**).

1225 **Mitochondria-specific flux, $J_{O_2/mtE}$:** Volume-specific metabolic O_2 flux depends on: (1)
 1226 the sample concentration in the volume of the instrument chamber, C_{mX} , or C_{NX} ; (2) the
 1227 mitochondrial density in the sample, $D_{mtE} = mtE/m_X$ or $mtE_X = mtE/N_X$; and (3) the specific
 1228 mitochondrial activity or performance per elemental mitochondrial unit, $J_{O_2/mtE} = J_{V,O_2}/C_{mtE}$
 1229 $[mol \cdot s^{-1} \cdot mtEU^{-1}]$ (**Table 4**). Obviously, the numerical results for $J_{O_2/mtE}$ vary with the type of
 1230 mitochondrial marker chosen for measurement of *mtE* and $C_{mtE} = mtE/V [mtEU \cdot m^{-3}]$.

1231

1232 3.5. Evaluation of mitochondrial markers

1233

1234 Different methods are implicated in the quantification of mitochondrial markers and have
 1235 different strengths. Some problems are common for all mitochondrial markers, *mtE*: (1)
 1236 Accuracy of measurement is crucial, since even a highly accurate and reproducible
 1237 measurement of O_2 flux results in an inaccurate and noisy expression if normalized by a biased
 1238 and noisy measurement of a mitochondrial marker. This problem is acute in mitochondrial
 1239 respiration because the denominators used (the mitochondrial markers) are often small moieties

1240 of which accurate and precise determination is difficult. This problem can be avoided when O₂
1241 fluxes measured in substrate-uncoupler-inhibitor titration protocols are normalized for flux in
1242 a defined respiratory reference state, which is used as an *internal* marker and yields flux control
1243 ratios, *FCRs*. *FCRs* are independent of *externally* measured markers and, therefore, are
1244 statistically robust, considering the limitations of ratios in general (Jasienski and Bazzaz 1999).
1245 *FCRs* indicate qualitative changes of mitochondrial respiratory control, with highest
1246 quantitative resolution, separating the effect of mitochondrial density or concentration on $J_{O_2/mX}$
1247 and $I_{O_2/X}$ from that of function per elemental mitochondrial marker, $J_{O_2/mtE}$ (Pesta *et al.* 2011;
1248 Gnaiger 2014). (2) If mitochondrial quality does not change and only the amount of
1249 mitochondria varies as a determinant of mass-specific flux, any marker is equally qualified in
1250 principle; then in practice selection of the optimum marker depends only on the accuracy and
1251 precision of measurement of the mitochondrial marker. (3) If mitochondrial flux control ratios
1252 change, then there may not be any best mitochondrial marker. In general, measurement of
1253 multiple mitochondrial markers enables a comparison and evaluation of normalization for a
1254 variety of mitochondrial markers. Particularly during postnatal development, the activity of
1255 marker enzymes—such as cytochrome *c* oxidase and citrate synthase—follows different time
1256 courses (Drahota *et al.* 2004). Evaluation of mitochondrial markers in healthy controls is
1257 insufficient for providing guidelines for application in the diagnosis of pathological states and
1258 specific treatments.

1259 In line with the concept of the respiratory control ratio (Chance and Williams 1955a), the
1260 most readily used normalization is that of flux control ratios and flux control factors (Gnaiger
1261 2014). Selection of the state of maximum flux in a protocol as the reference state has the
1262 advantages of: (1) internal normalization; (2) statistical linearization of the response in the range
1263 of 0 to 1; and (3) consideration of maximum flux for integrating a large number of elemental
1264 steps in the OXPHOS- or ET-pathways. This reduces the risk of selecting a functional marker
1265 that is specifically altered by the treatment or pathology, yet increases the chance that the highly
1266 integrative pathway is disproportionately affected, *e.g.*, the OXPHOS- rather than ET-pathway
1267 in case of an enzymatic defect in the phosphorylation-pathway. In this case, additional
1268 information can be obtained by reporting flux control ratios based on a reference state which
1269 indicates stable tissue-mass specific flux. Stereological determination of mitochondrial content
1270 via two-dimensional transmission electron microscopy can have limitations due to the dynamics
1271 of mitochondrial size (Meinild Lundby *et al.* 2017). Accurate determination of three-
1272 dimensional volume by two-dimensional microscopy can be both time consuming and
1273 statistically challenging (Larsen *et al.* 2012).

1274 The validity of using mitochondrial marker enzymes (citrate synthase activity, Complex
1275 I–IV amount or activity) for normalization of flux is limited in part by the same factors that
1276 apply to flux control ratios. Strong correlations between various mitochondrial markers and
1277 citrate synthase activity (Reichmann *et al.* 1985; Boushel *et al.* 2007; Mogensen *et al.* 2007)
1278 are expected in a specific tissue of healthy persons and in disease states not specifically
1279 targeting citrate synthase. Citrate synthase activity is acutely modifiable by exercise
1280 (Tonkonogi *et al.* 1997; Leek *et al.* 2001). Evaluation of mitochondrial markers related to a
1281 selected age and sex cohort cannot be extrapolated to provide recommendations for
1282 normalization in respirometric diagnosis of disease, in different states of development and
1283 ageing, different cell types, tissues, and species. mtDNA normalized to nDNA via qPCR is
1284 correlated to functional mitochondrial markers including OXPHOS- and ET-capacity in some
1285 cases (Puntschart *et al.* 1995; Wang *et al.* 1999; Menshikova *et al.* 2006; Boushel *et al.* 2007),
1286 but lack of such correlations have been reported (Menshikova *et al.* 2005; Schultz and Wiesner
1287 2000; Pesta *et al.* 2011). Several studies indicate a strong correlation between cardiolipin
1288 content and increase in mitochondrial function with exercise (Menshikova *et al.* 2005;
1289 Menshikova *et al.* 2007; Larsen *et al.* 2012; Faber *et al.* 2014), but it has not been evaluated as
1290 a general mitochondrial biomarker in disease. With no single best mitochondrial marker, a good

1291 strategy is to quantify several different biomarkers to minimize the decorrelating effects caused
 1292 by diseases, treatments, or other factors.

1293

1294 3.6. Conversion: units

1295

1296 Many different units have been used to report the O₂ consumption rate, OCR (**Table 6**).
 1297 *SI* base units provide the common reference to introduce the theoretical principles (**Figure 7**),
 1298 and are used with appropriately chosen *SI* prefixes to express numerical data in the most
 1299 practical format, with an effort towards unification within specific areas of application (**Table**
 1300 **7**). Reporting data in *SI* units—including the mole [mol], coulomb [C], joule [J], and second
 1301 [s]—should be encouraged, particularly by journals which propose the use of *SI* units.

1302

1303 **Table 6. Conversion of various units used in respirometry and**
 1304 **ergometry.** e^- is the number of electrons or reducing equivalents. z_B is the
 1305 charge number of entity B.

1 Unit		Multiplication factor	<i>SI</i> -unit	Note
ng.atom O·s ⁻¹	(2 e ⁻)	0.5	nmol O ₂ ·s ⁻¹	
ng.atom O·min ⁻¹	(2 e ⁻)	8.33	pmol O ₂ ·s ⁻¹	
natom O·min ⁻¹	(2 e ⁻)	8.33	pmol O ₂ ·s ⁻¹	
nmol O ₂ ·min ⁻¹	(4 e ⁻)	16.67	pmol O ₂ ·s ⁻¹	
nmol O ₂ ·h ⁻¹	(4 e ⁻)	0.2778	pmol O ₂ ·s ⁻¹	
mL O ₂ ·min ⁻¹ at STPD ^a		0.744	μmol O ₂ ·s ⁻¹	1
W = J/s at -470 kJ/mol O ₂		-2.128	μmol O ₂ ·s ⁻¹	
mA = mC·s ⁻¹	(z _{H+} = 1)	10.36	nmol H ⁺ ·s ⁻¹	2
mA = mC·s ⁻¹	(z _{O₂} = 4)	2.59	nmol O ₂ ·s ⁻¹	2
nmol H ⁺ ·s ⁻¹	(z _{H+} = 1)	0.09649	mA	3
nmol O ₂ ·s ⁻¹	(z _{O₂} = 4)	0.38594	mA	3

1307

1308

1309

1310

1311

1312

1313

1314

1315

- 1 At standard temperature and pressure dry (STPD: 0 °C = 273.15 K and 1 atm = 101.325 kPa = 760 mmHg), the molar volume of an ideal gas, V_m , and V_{m,O_2} is 22.414 and 22.392 L·mol⁻¹, respectively. Rounded to three decimal places, both values yield the conversion factor of 0.744. For comparison at normal temperature and pressure dry (NTPD: 20 °C), V_{m,O_2} is 24.038 L·mol⁻¹. Note that the *SI* standard pressure is 100 kPa.
- 2 The multiplication factor is $10^6/(z_B \cdot F)$.
- 3 The multiplication factor is $z_B \cdot F/10^6$.

1316

1317

1318

1319

1320

1321

1322

1323

1324

1325

1326

1327

Although volume is expressed as m³ using the *SI* base unit, the litre [dm³] is a conventional unit of volume for concentration and is used for most solution chemical kinetics. If one multiplies $I_{O_2/cell}$ by C_{Ncell} , then the result will not only be the amount of O₂ [mol] consumed per time [s⁻¹] in one litre [L⁻¹], but also the change in O₂ concentration per second (for any volume of an ideally closed system). This is ideal for kinetic modeling as it blends with chemical rate equations where concentrations are typically expressed in mol·L⁻¹ (Wagner *et al.* 2011). In studies of multinuclear cells—such as differentiated skeletal muscle cells—it is easy to determine the number of nuclei but not the total number of cells. A generalized concept, therefore, is obtained by substituting cells by nuclei as the sample entity. This does not hold, however, for enucleated platelets.

For studies of cells, we recommend that respiration be expressed, as far as possible, as: (*I*) O₂ flux normalized for a mitochondrial marker, for separation of the effects of mitochondrial

1328 quality and content on cell respiration (this includes *FCRs* as a normalization for a functional
 1329 mitochondrial marker); (2) O_2 flux in units of cell volume or mass, for comparison of respiration
 1330 of cells with different cell size (Renner *et al.* 2003) and with studies on tissue preparations, and
 1331 (3) O_2 flow in units of attomole (10^{-18} mol) of O_2 consumed in a second by each cell
 1332 [$\text{amol}\cdot\text{s}^{-1}\cdot\text{cell}^{-1}$], numerically equivalent to [$\text{pmol}\cdot\text{s}^{-1}\cdot 10^{-6}$ cells]. This convention allows
 1333 information to be easily used when designing experiments in which O_2 flow must be considered.
 1334 For example, to estimate the volume-specific O_2 flux in an instrument chamber that would be
 1335 expected at a particular cell number concentration, one simply needs to multiply the flow per
 1336 cell by the number of cells per volume of interest. This provides the amount of O_2 [mol]
 1337 consumed per time [s^{-1}] per unit volume [L^{-1}]. At an O_2 flow of $100 \text{ amol}\cdot\text{s}^{-1}\cdot\text{cell}^{-1}$ and a cell
 1338 density of $10^9 \text{ cells}\cdot\text{L}^{-1}$ ($10^6 \text{ cells}\cdot\text{mL}^{-1}$), the volume-specific O_2 flux is $100 \text{ nmol}\cdot\text{s}^{-1}\cdot\text{L}^{-1}$ (100
 1339 $\text{pmol}\cdot\text{s}^{-1}\cdot\text{mL}^{-1}$).

1340
1341

Table 7. Conversion of units with preservation of numerical values.

Name	Frequently used unit	Equivalent unit	Note
volume-specific flux, J_{V,O_2}	$\text{pmol}\cdot\text{s}^{-1}\cdot\text{mL}^{-1}$ $\text{mmol}\cdot\text{s}^{-1}\cdot\text{L}^{-1}$	$\text{nmol}\cdot\text{s}^{-1}\cdot\text{L}^{-1}$ $\text{mol}\cdot\text{s}^{-1}\cdot\text{m}^{-3}$	1
cell-specific flow, $I_{O_2/\text{cell}}$	$\text{pmol}\cdot\text{s}^{-1}\cdot 10^{-6}$ cells	$\text{amol}\cdot\text{s}^{-1}\cdot\text{cell}^{-1}$	2
	$\text{pmol}\cdot\text{s}^{-1}\cdot 10^{-9}$ cells	$\text{zmol}\cdot\text{s}^{-1}\cdot\text{cell}^{-1}$	3
cell number concentration, C_{Nce}	$10^6 \text{ cells}\cdot\text{mL}^{-1}$	$10^9 \text{ cells}\cdot\text{L}^{-1}$	
mitochondrial protein concentration, C_{mtE}	$0.1 \text{ mg}\cdot\text{mL}^{-1}$	$0.1 \text{ g}\cdot\text{L}^{-1}$	
mass-specific flux, $J_{O_2/m}$	$\text{pmol}\cdot\text{s}^{-1}\cdot\text{mg}^{-1}$	$\text{nmol}\cdot\text{s}^{-1}\cdot\text{g}^{-1}$	4
catabolic power, P_k	$\mu\text{W}\cdot 10^{-6}$ cells	$\text{pW}\cdot\text{cell}^{-1}$	1
Volume	1,000 L	m^3 (1,000 kg)	
	L	dm^3 (kg)	
	mL	cm^3 (g)	
	μL	mm^3 (mg)	
	fL	μm^3 (pg)	5
amount of substance concentration	$\text{M} = \text{mol}\cdot\text{L}^{-1}$	$\text{mol}\cdot\text{dm}^{-3}$	

1342
1343
1344
1345
1346

- | | | | |
|---|----------------------------------|---|--------------------------------|
| 1 | pmol: picomole = 10^{-12} mol | 4 | nmol: nanomole = 10^{-9} mol |
| 2 | amol: attomole = 10^{-18} mol | 5 | fL: femtolitre = 10^{-15} L |
| 3 | zmol: zeptomole = 10^{-21} mol | | |

1347 ET-capacity in human cell types including HEK 293, primary HUVEC and fibroblasts
 1348 ranges from 50 to $180 \text{ amol}\cdot\text{s}^{-1}\cdot\text{cell}^{-1}$, measured in intact cells in the noncoupled state (see
 1349 Gnaiger 2014). At $100 \text{ amol}\cdot\text{s}^{-1}\cdot\text{cell}^{-1}$ corrected for *Rox*, the current across the mt-membranes,
 1350 I_{H^+e} , approximates $193 \text{ pA}\cdot\text{cell}^{-1}$ or 0.2 nA per cell. See Rich (2003) for an extension of
 1351 quantitative bioenergetics from the molecular to the human scale, with a transmembrane proton
 1352 flux equivalent to 520 A in an adult at a catabolic power of -110 W. Modelling approaches
 1353 illustrate the link between protonmotive force and currents (Willis *et al.* 2016).

1354 We consider isolated mitochondria as powerhouses and proton pumps as molecular
 1355 machines to relate experimental results to energy metabolism of the intact cell. The cellular
 1356 P_{\gg}/O_2 based on oxidation of glycogen is increased by the glycolytic (fermentative) substrate-
 1357 level phosphorylation of 3 P_{\gg}/Glyc or 0.5 mol P_{\gg} for each mol O_2 consumed in the complete
 1358 oxidation of a mol glycosyl unit (Glyc). Adding 0.5 to the mitochondrial P_{\gg}/O_2 ratio of 5.4
 1359 yields a bioenergetic cell physiological P_{\gg}/O_2 ratio close to 6. Two NADH equivalents are
 1360 formed during glycolysis and transported from the cytosol into the mitochondrial matrix, either
 1361 by the malate-aspartate shuttle or by the glycerophosphate shuttle (**Figure 2A**) resulting in

different theoretical yields of ATP generated by mitochondria, the energetic cost of which potentially must be taken into account. Considering also substrate-level phosphorylation in the TCA cycle, this high P_{O_2}/O_2 ratio not only reflects proton translocation and OXPHOS studied in isolation, but integrates mitochondrial physiology with energy transformation in the living cell (Gnaiger 1993a).

4. Conclusions

Catabolic cell respiration is the process of exergonic and exothermic energy transformation in which scalar redox reactions are coupled to vectorial ion translocation across a semipermeable membrane, which separates the small volume of a bacterial cell or mitochondrion from the larger volume of its surroundings. The electrochemical exergy can be partially conserved in the phosphorylation of ADP to ATP or in ion pumping, or dissipated in an electrochemical short-circuit. Respiration is thus clearly distinguished from fermentation as the counterpart of cellular core energy metabolism. An O_2 flux balance scheme illustrates the relationships and general definitions (**Figures 1 and 2**).

Experimentally, respiration is separated in mitochondrial preparations from the interactions with the fermentative pathways of the intact cell. OXPHOS analysis (**Figure 3**) is based on the study of mitochondrial preparations complementary to bioenergetic investigations of intact cells and organisms—from model organisms to the human species including healthy and diseased persons (patients). Different mechanisms of respiratory uncoupling have to be distinguished (**Figure 4**). Metabolic fluxes measured in defined coupling and pathway control states (**Figures 5 and 6**) provide insights into the meaning of cellular and organismic respiration.

The optimal choice for expressing mitochondrial and cell respiration as O_2 flow per biological sample, and normalization for specific tissue-markers (volume, mass, protein) and mitochondrial markers (volume, protein, content, mtDNA, activity of marker enzymes, respiratory reference state) is guided by the scientific question under study. Interpretation of the data depends critically on appropriate normalization (**Figure 7**).

MitoEAGLE can serve as a gateway to better diagnose mitochondrial respiratory defects linked to genetic variation, age-related health risks, sex-specific mitochondrial performance, lifestyle with its effects on degenerative diseases, and thermal and chemical environment. The present recommendations on coupling control states and rates, linked to the concept of the protonmotive force, are focused on studies with mitochondrial preparations (**Box 3**). These will be extended in a series of reports on pathway control of mitochondrial respiration, respiratory states in intact cells, and harmonization of experimental procedures.

Box 3: Recommendations for studies with mitochondrial preparations

- Normalization of respiratory rates should be provided as far as possible:
 1. *Biophysical normalization*: on a per cell basis as O_2 flow; this may not be possible when dealing with coenocytic organisms or tissues without cross-walls separating individual cells (e.g., filamentous fungi, muscle fibers)
 2. *Cellular normalization*: per g protein; per cell- or tissue-mass as mass-specific O_2 flux; per cell volume as cell volume-specific flux
 3. *Mitochondrial normalization*: per mitochondrial marker as mt-specific flux.

With information on cell size and the use of multiple normalizations, maximum potential information is available (Renner *et al.* 2003; Wagner *et al.* 2011; Gnaiger 2014). Reporting

- 1412 flow in a respiratory chamber [$\text{nmol}\cdot\text{s}^{-1}$] is discouraged, since it restricts the analysis to intra-
 1413 experimental comparison of relative (qualitative) differences.
- 1414 ● Catabolic mitochondrial respiration is distinguished from residual O_2 consumption. Fluxes
 1415 in mitochondrial coupling states should be, as far as possible, corrected for residual O_2
 1416 consumption.
 - 1417 ● Different mechanisms of uncoupling should be distinguished by defined terms. The tightness
 1418 of coupling relates to these uncoupling mechanisms, whereas the coupling stoichiometry
 1419 varies as a function the substrate type involved in ET-pathways with either three or two
 1420 redox proton pumps operating in series. Separation of tightness of coupling from the
 1421 pathway-dependent coupling stoichiometry is possible only when the substrate type
 1422 undergoing oxidation remains the same for respiration in LEAK-, OXPHOS-, and ET-states.
 1423 In studies of the tightness of coupling, therefore, simple substrate-inhibitor combinations
 1424 should be applied to exclude a shift in substrate competition which may occur when
 1425 providing physiological substrate cocktails.
 - 1426 ● In studies of isolated mitochondria, the mitochondrial recovery and yield should be reported.
 1427 Experimental criteria for evaluation of purity versus integrity should be considered.
 1428 Mitochondrial markers—such as citrate synthase activity as an enzymatic matrix marker—
 1429 provide a link to the tissue of origin on the basis of calculating the mitochondrial recovery,
 1430 *i.e.*, the fraction of mitochondrial marker obtained from a unit mass of tissue. Total
 1431 mitochondrial protein is frequently applied as a mitochondrial marker, which is restricted to
 1432 isolated mitochondria.
 - 1433 ● In studies of permeabilized cells, the viability of the cell culture or cell suspension of origin
 1434 should be reported. Normalization should be evaluated for total cell count or viable cell
 1435 count.
 - 1436 ● Terms and symbols are summarized in **Table 8**. Their use will facilitate transdisciplinary
 1437 communication and support further developments towards a consistent theory of
 1438 bioenergetics and mitochondrial physiology. Technical terms related to and defined with
 1439 normal words can be used as index terms in databases, support the creation of ontologies
 1440 towards semantic information processing (MitoPedia), and help in communicating analytical
 1441 findings as impactful data-driven stories. ‘*Making data available without making it*
 1442 *understandable may be worse than not making it available at all*’ (National Academies of
 1443 Sciences, Engineering, and Medicine 2018). Success will depend on taking next steps: (1)
 1444 exhaustive text-mining considering Omics data and functional data; (2) network analysis of
 1445 Omics data with bioinformatics tools; (3) cross-validation with distinct bioinformatics
 1446 approaches; (4) correlation with functional data; (5) guidelines for biological validation of
 1447 network data. This is a call to carefully contribute to FAIR principles (Findable, Accessible,
 1448 Interoperable, Reusable) for the sharing of scientific data.

1450
 1451
 1452 **Table 8. Terms, symbols, and units.**
 1453
 1454

1455 Term	1456 Symbol	1457 Unit	1458 Links and comments
1459 alternative quinol oxidase	1460 AOX		1461 Figure 2B
1462 amount of substance B	1463 n_B	1464 [mol]	
1465 ATP yield per O_2	1466 $Y_{P\gg/O_2}$		1467 $P\gg/O_2$ ratio measured in any respiratory 1468 state
1469 catabolic reaction	1470 k		1471 Figure 1 and 3
1472 catabolic respiration	1473 J_{kO_2}	1474 <i>varies</i>	1475 Figure 1 and 3
1476 cell number	1477 N_{cell}	1478 [x]	1479 Table 5; $N_{\text{cell}} = N_{\text{vce}} + N_{\text{dce}}$
1480 cell respiration	1481 J_{rO_2}	1482 <i>varies</i>	1483 Figure 1
1484 cell viability index	1485 CVI		1486 $CVI = N_{\text{vce}}/N_{\text{cell}} = 1 - N_{\text{dce}}/N_{\text{cell}}$

1467	Complexes I to IV	CI to CIV		respiratory ET Complexes; Figure 2B
1468	concentration of substance B	$c_B = n_B \cdot V^{-1}$; [B]	[mol·m ⁻³]	Box 2
1469	dead cell number	N_{dce}	[x]	Table 5; non-viable cells, loss of plasma membrane barrier function
1470				
1471	electron transfer system	ETS		Figure 2B, Figure 5; state
1472	flow, for substance B	I_B	[mol·s ⁻¹]	system-related extensive quantity; Figure 7
1473				
1474	flux, for substance B	J_B	<i>varies</i>	size-specific quantity; Figure 7
1475	inorganic phosphate	P_i		Figure 3
1476	intact cell number, viable cell number	N_{vce}	[x]	Table 5; viable cells, intact of plasma membrane barrier function
1477				
1478	LEAK	LEAK		Table 1, Figure 5; state
1479	mass of sample X	m_X	[kg]	Table 4
1480	mass of entity X	M_X	[kg]	mass of object X; Table 4
1481	MITOCARTA			https://www.broadinstitute.org/scientific-community/science/programs/metabolic-disease-program/publications/mitocarta/mitocarta-in-0
1482				
1483				
1484				
1485				
1486	MitoPedia			http://www.bioblast.at/index.php/MitoPedia
1487	mitochondria or mitochondrial	mt		Box 1
1488	mitochondrial DNA	mtDNA		Box 1
1489	mitochondrial concentration	$C_{mtE} = mtE \cdot V^{-1}$	[mtEU·m ⁻³]	Table 4
1490	mitochondrial content	$mtE_X = mtE \cdot N_X^{-1}$	[mtEU·x ⁻¹]	Table 4
1491	mitochondrial elemental unit	mtEU	<i>varies</i>	Table 4, specific units for mt-marker
1492	mitochondrial inner membrane	mtIM		Figure 2; MIM is widely used; the first M is replaced by mt; Box 1
1493				
1494	mitochondrial outer membrane	mtOM		Figure 2; MOM is widely used; the first M is replaced by mt; Box 1
1495				
1496	mitochondrial recovery	Y_{mtE}		fraction of <i>mtE</i> recovered in sample from the tissue of origin
1497				
1498	mitochondrial yield	$Y_{mtE/m}$		$Y_{mtE/m} = Y_{mtE} \cdot D_{mtE}$
1499	negative	neg		Figure 3
1500	number concentration of X	C_{NX}	[x·m ⁻³]	Table 4
1501	number of entities X	N_X	[x]	Table 4, Figure 7
1502	number of entity B	N_B	[x]	Table 4
1503	oxidative phosphorylation	OXPPOS		Table 1, Figure 5; state
1504	oxygen concentration	$c_{O_2} = n_{O_2} \cdot V^{-1}$; [O ₂]	[mol·m ⁻³]	Section 3.2
1505	oxygen flux, in reaction r	J_{rO_2}	<i>varies</i>	Figure 1
1506	permeabilized cell number	N_{pcc}	[x]	Table 5; experimental permeabilization of plasma membrane; $N_{pcc} = N_{cell}$
1507				
1508	phosphorylation of ADP to ATP	P»		Section 2.2
1509	positive	pos		Figure 3
1510	proton in the negative compartment	H ⁺ _{neg}		Figure 3
1511	proton in the positive compartment	H ⁺ _{pos}		Figure 3
1512	rate of electron transfer in ET state	E		ET-capacity; Table 1
1513	rate of LEAK respiration	L		Table 1
1514	rate of oxidative phosphorylation	P		OXPPOS capacity; Table 1
1515	rate of residual oxygen consumption	Rox		Table 1, Figure 1
1516	residual oxygen consumption	ROX		Table 1; state
1517	respiratory supercomplex	SC I _n III _n IV _n		Box 1; supramolecular assemblies composed of variable copy numbers (<i>n</i>) of CI, CIII and CIV
1518				
1519				
1520	specific mitochondrial density	$D_{mtE} = mtE \cdot m_X^{-1}$	[mtEU·kg ⁻¹]	Table 4
1521	volume	V	[m ⁻³]	Table 7
1522	weight, dry weight	W_d	[kg]	used as mass of sample X; Figure 7
1523	weight, wet weight	W_w	[kg]	used as mass of sample X; Figure 7
1524				
1525				
1526				

1527 **Acknowledgements**

1528 We thank M. Beno for management assistance. This publication is based upon work from COST
1529 Action CA15203 MitoEAGLE, supported by COST (European Cooperation in Science and
1530 Technology), and K-Regio project MitoFit (E.G.).

1531
1532 **Competing financial interests:** E.G. is founder and CEO of Oroboros Instruments, Innsbruck,
1533 Austria.

1534
1535 **References**

- 1536
1537 Altmann R (1894) Die Elementarorganismen und ihre Beziehungen zu den Zellen. Zweite vermehrte Auflage.
1538 Verlag Von Veit & Comp, Leipzig:160 pp.
- 1539 Beard DA (2005) A biophysical model of the mitochondrial respiratory system and oxidative phosphorylation.
1540 PLoS Comput Biol 1(4):e36.
- 1541 Benda C (1898) Weitere Mitteilungen über die Mitochondria. Verh Dtsch Physiol Ges:376-83.
- 1542 Birkedal R, Laasmaa M, Vendelin M (2014) The location of energetic compartments affects energetic
1543 communication in cardiomyocytes. Front Physiol 5:376.
- 1544 Breton S, Beaupré HD, Stewart DT, Hoeh WR, Blier PU (2007) The unusual system of doubly uniparental
1545 inheritance of mtDNA: isn't one enough? Trends Genet 23:465-74.
- 1546 Brown GC (1992) Control of respiration and ATP synthesis in mammalian mitochondria and cells. Biochem J
1547 284:1-13.
- 1548 Calvo SE, Klausner CR, Mootha VK (2016) MitoCarta2.0: an updated inventory of mammalian mitochondrial
1549 proteins. Nucleic Acids Research 44:D1251-7.
- 1550 Calvo SE, Julien O, Clauser KR, Shen H, Kamer KJ, Wells JA, Mootha VK (2017) Comparative analysis of
1551 mitochondrial N-termini from mouse, human, and yeast. Mol Cell Proteomics 16:512-23.
- 1552 Campos JC, Queliconi BB, Bozi LHM, Bechara LRG, Dourado PMM, Andres AM, Jannig PR, Gomes KMS,
1553 Zambelli VO, Rocha-Resende C, Guatimosim S, Brum PC, Mochly-Rosen D, Gottlieb RA, Kowaltowski AJ,
1554 Ferreira JCB (2017) Exercise reestablishes autophagic flux and mitochondrial quality control in heart failure.
1555 Autophagy 13:1304-317.
- 1556 Canton M, Luvisetto S, Schmehl I, Azzone GF (1995) The nature of mitochondrial respiration and
1557 discrimination between membrane and pump properties. Biochem J 310:477-81.
- 1558 Carrico C, Meyer JG, He W, Gibson BW, Verdin E (2018) The mitochondrial acylome emerges: proteomics,
1559 regulation by Sirtuins, and metabolic and disease implications. Cell Metab 27:497-512.
- 1560 Chance B, Williams GR (1955a) Respiratory enzymes in oxidative phosphorylation. I. Kinetics of oxygen
1561 utilization. J Biol Chem 217:383-93.
- 1562 Chance B, Williams GR (1955b) Respiratory enzymes in oxidative phosphorylation: III. The steady state. J Biol
1563 Chem 217:409-27.
- 1564 Chance B, Williams GR (1955c) Respiratory enzymes in oxidative phosphorylation. IV. The respiratory chain. J
1565 Biol Chem 217:429-38.
- 1566 Chance B, Williams GR (1956) The respiratory chain and oxidative phosphorylation. Adv Enzymol Relat Subj
1567 Biochem 17:65-134.
- 1568 Cobb LJ, Lee C, Xiao J, Yen K, Wong RG, Nakamura HK, Mehta HH, Gao Q, Ashur C, Huffman DM, Wan J,
1569 Muzumdar R, Barzilai N, Cohen P (2016) Naturally occurring mitochondrial-derived peptides are age-
1570 dependent regulators of apoptosis, insulin sensitivity, and inflammatory markers. Aging (Albany NY) 8:796-
1571 809.
- 1572 Cohen ER, Cvitas T, Frey JG, Holmström B, Kuchitsu K, Marquardt R, Mills I, Pavese F, Quack M, Stohner J,
1573 Strauss HL, Takami M, Thor HL (2008) Quantities, units and symbols in physical chemistry, IUPAC Green
1574 Book, 3rd Edition, 2nd Printing, IUPAC & RSC Publishing, Cambridge.
- 1575 Cooper H, Hedges LV, Valentine JC, eds (2009) The handbook of research synthesis and meta-analysis. Russell
1576 Sage Foundation.
- 1577 Coopersmith J (2010) Energy, the subtle concept. The discovery of Feynman's blocks from Leibnitz to Einstein.
1578 Oxford University Press:400 pp.
- 1579 Cummins J (1998) Mitochondrial DNA in mammalian reproduction. Rev Reprod 3:172-82.
- 1580 Dai Q, Shah AA, Garde RV, Yonish BA, Zhang L, Medvitz NA, Miller SE, Hansen EL, Dunn CN, Price TM
1581 (2013) A truncated progesterone receptor (PR-M) localizes to the mitochondrion and controls cellular
1582 respiration. Mol Endocrinol 27:741-53.
- 1583 Daum B, Walter A, Horst A, Osiewacz HD, Kühlbrandt W (2013) Age-dependent dissociation of ATP synthase
1584 dimers and loss of inner-membrane cristae in mitochondria. Proc Natl Acad Sci U S A 110:15301-6.
- 1585 Divakaruni AS, Brand MD (2011) The regulation and physiology of mitochondrial proton leak. Physiology
1586 (Bethesda) 26:192-205.

- 1587 Doerrier C, Garcia-Souza LF, Krumschnabel G, Wohlfarter Y, Mészáros AT, Gnaiger E (2018) High-Resolution
 1588 FluoRespirometry and OXPHOS protocols for human cells, permeabilized fibres from small biopsies of
 1589 muscle, and isolated mitochondria. *Methods Mol Biol* 1782 (Palmeira CM, Moreno AJ, eds): Mitochondrial
 1590 Bioenergetics, 978-1-4939-7830-4.
- 1591 Doskey CM, van 't Erve TJ, Wagner BA, Buettner GR (2015) Moles of a substance per cell is a highly
 1592 informative dosing metric in cell culture. *PLOS ONE* 10:e0132572.
- 1593 Drahotka Z, Milerová M, Stieglarová A, Houstek J, Ostádal B (2004) Developmental changes of cytochrome *c*
 1594 oxidase and citrate synthase in rat heart homogenate. *Physiol Res* 53:119-22.
- 1595 Duarte FV, Palmeira CM, Rolo AP (2014) The role of microRNAs in mitochondria: small players acting wide.
 1596 *Genes (Basel)* 5:865-86.
- 1597 Ernster L, Schatz G (1981) Mitochondria: a historical review. *J Cell Biol* 91:227s-55s.
- 1598 Estabrook RW (1967) Mitochondrial respiratory control and the polarographic measurement of ADP:O ratios.
 1599 *Methods Enzymol* 10:41-7.
- 1600 Faber C, Zhu ZJ, Castellino S, Wagner DS, Brown RH, Peterson RA, Gates L, Barton J, Bickett M, Hagerty L,
 1601 Kimbrough C, Sola M, Bailey D, Jordan H, Elangbam CS (2014) Cardiolipin profiles as a potential
 1602 biomarker of mitochondrial health in diet-induced obese mice subjected to exercise, diet-restriction and
 1603 ephedrine treatment. *J Appl Toxicol* 34:1122-9.
- 1604 Fell D (1997) Understanding the control of metabolism. Portland Press.
- 1605 Garlid KD, Beavis AD, Ratkje SK (1989) On the nature of ion leaks in energy-transducing membranes. *Biochim*
 1606 *Biophys Acta* 976:109-20.
- 1607 Garlid KD, Semrad C, Zinchenko V. Does redox slip contribute significantly to mitochondrial respiration? In:
 1608 Schuster S, Rigoulet M, Ouhabi R, Mazat J-P, eds (1993) *Modern trends in biothermokinetics*. Plenum Press,
 1609 New York, London:287-93.
- 1610 Gerö D, Szabo C (2016) Glucocorticoids suppress mitochondrial oxidant production via upregulation of
 1611 uncoupling protein 2 in hyperglycemic endothelial cells. *PLoS One* 11:e0154813.
- 1612 Gnaiger E. Efficiency and power strategies under hypoxia. Is low efficiency at high glycolytic ATP production a
 1613 paradox? In: *Surviving Hypoxia: Mechanisms of Control and Adaptation*. Hochachka PW, Lutz PL, Sick T,
 1614 Rosenthal M, Van den Thillart G, eds (1993a) CRC Press, Boca Raton, Ann Arbor, London, Tokyo:77-109.
- 1615 Gnaiger E (1993b) Nonequilibrium thermodynamics of energy transformations. *Pure Appl Chem* 65:1983-2002.
- 1616 Gnaiger E (2001) Bioenergetics at low oxygen: dependence of respiration and phosphorylation on oxygen and
 1617 adenosine diphosphate supply. *Respir Physiol* 128:277-97.
- 1618 Gnaiger E (2009) Capacity of oxidative phosphorylation in human skeletal muscle. *New perspectives of*
 1619 *mitochondrial physiology*. *Int J Biochem Cell Biol* 41:1837-45.
- 1620 Gnaiger E (2014) Mitochondrial pathways and respiratory control. An introduction to OXPHOS analysis. 4th ed.
 1621 *Mitochondr Physiol Network* 19.12. Oroboros MiPNet Publications, Innsbruck:80 pp.
- 1622 Gnaiger E, Méndez G, Hand SC (2000) High phosphorylation efficiency and depression of uncoupled respiration
 1623 in mitochondria under hypoxia. *Proc Natl Acad Sci USA* 97:11080-5.
- 1624 Greggio C, Jha P, Kulkarni SS, Lagarrigue S, Broskey NT, Boutant M, Wang X, Conde Alonso S, Ofori E,
 1625 Auwerx J, Cantó C, Amati F (2017) Enhanced respiratory chain supercomplex formation in response to
 1626 exercise in human skeletal muscle. *Cell Metab* 25:301-11.
- 1627 Hinkle PC (2005) P/O ratios of mitochondrial oxidative phosphorylation. *Biochim Biophys Acta* 1706:1-11.
- 1628 Hofstadter DR (1979) Gödel, Escher, Bach: An eternal golden braid. A metaphorical fugue on minds and
 1629 machines in the spirit of Lewis Carroll. Harvester Press:499 pp.
- 1630 Illaste A, Laasmaa M, Peterson P, Vendelin M (2012) Analysis of molecular movement reveals latticelike
 1631 obstructions to diffusion in heart muscle cells. *Biophys J* 102:739-48.
- 1632 Jasienski M, Bazzaz FA (1999) The fallacy of ratios and the testability of models in biology. *Oikos* 84:321-26.
- 1633 Jepihhina N, Beraud N, Sepp M, Birkedal R, Vendelin M (2011) Permeabilized rat cardiomyocyte response
 1634 demonstrates intracellular origin of diffusion obstacles. *Biophys J* 101:2112-21.
- 1635 Klepinin A, Ounpuu L, Guzun R, Chekulayev V, Timohhina N, Tepp K, Shevchuk I, Schlattner U, Kaambre T
 1636 (2016) Simple oxygraphic analysis for the presence of adenylate kinase 1 and 2 in normal and tumor cells. *J*
 1637 *Bioenerg Biomembr* 48:531-48.
- 1638 Klingenberg M (2017) UCP1 - A sophisticated energy valve. *Biochimie* 134:19-27.
- 1639 Koit A, Shevchuk I, Ounpuu L, Klepinin A, Chekulayev V, Timohhina N, Tepp K, Puurand M, Truu L, Heck K,
 1640 Valvere V, Guzun R, Kaambre T (2017) Mitochondrial respiration in human colorectal and breast cancer
 1641 clinical material is regulated differently. *Oxid Med Cell Longev* 1372640.
- 1642 Komlódi T, Tretter L (2017) Methylene blue stimulates substrate-level phosphorylation catalysed by succinyl-
 1643 CoA ligase in the citric acid cycle. *Neuropharmacology* 123:287-98.
- 1644 Lane N (2005) Power, sex, suicide: mitochondria and the meaning of life. Oxford University Press:354 pp.
- 1645 Larsen S, Nielsen J, Neigaard Nielsen C, Nielsen LB, Wibrand F, Stride N, Schroder HD, Boushel RC, Helge
 1646 JW, Dela F, Hey-Mogensen M (2012) Biomarkers of mitochondrial content in skeletal muscle of healthy
 1647 young human subjects. *J Physiol* 590:3349-60.

- 1648 Lee C, Zeng J, Drew BG, Sallam T, Martin-Montalvo A, Wan J, Kim SJ, Mehta H, Hevener AL, de Cabo R,
1649 Cohen P (2015) The mitochondrial-derived peptide MOTS-c promotes metabolic homeostasis and reduces
1650 obesity and insulin resistance. *Cell Metab* 21:443-54.
- 1651 Lee SR, Kim HK, Song IS, Youm J, Dizon LA, Jeong SH, Ko TH, Heo HJ, Ko KS, Rhee BD, Kim N, Han J
1652 (2013) Glucocorticoids and their receptors: insights into specific roles in mitochondria. *Prog Biophys Mol*
1653 *Biol* 112:44-54.
- 1654 Leek BT, Mudaliar SR, Henry R, Mathieu-Costello O, Richardson RS (2001) Effect of acute exercise on citrate
1655 synthase activity in untrained and trained human skeletal muscle. *Am J Physiol Regul Integr Comp Physiol*
1656 280:R441-7.
- 1657 Lemieux H, Blier PU, Gnaiger E (2017) Remodeling pathway control of mitochondrial respiratory capacity by
1658 temperature in mouse heart: electron flow through the Q-junction in permeabilized fibers. *Sci Rep* 7:2840.
- 1659 Lenaz G, Tioli G, Falasca AI, Genova ML (2017) Respiratory supercomplexes in mitochondria. In: *Mechanisms*
1660 *of primary energy trasduction in biology*. M Wikstrom (ed) Royal Society of Chemistry Publishing, London,
1661 UK:296-337.
- 1662 Liu S, Roellig DM, Guo Y, Li N, Frace MA, Tang K, Zhang L, Feng Y, Xiao L (2016) Evolution of mitosome
1663 metabolism and invasion-related proteins in *Cryptosporidium*. *BMC Genomics* 17:1006.
- 1664 Margulis L (1970) *Origin of eukaryotic cells*. New Haven: Yale University Press.
- 1665 Meinild Lundby AK, Jacobs RA, Gehrig S, de Leur J, Hauser M, Bonne TC, Flück D, Dandanell S, Kirk N,
1666 Kaech A, Ziegler U, Larsen S, Lundby C (2018) Exercise training increases skeletal muscle mitochondrial
1667 volume density by enlargement of existing mitochondria and not de novo biogenesis. *Acta Physiol* 222,
1668 e12905.
- 1669 Menshikova EV, Ritov VB, Fairfull L, Ferrell RE, Kelley DE, Goodpaster BH (2006) Effects of exercise on
1670 mitochondrial content and function in aging human skeletal muscle. *J Gerontol A Biol Sci Med Sci* 61:534-
1671 40.
- 1672 Menshikova EV, Ritov VB, Ferrell RE, Azuma K, Goodpaster BH, Kelley DE (2007) Characteristics of skeletal
1673 muscle mitochondrial biogenesis induced by moderate-intensity exercise and weight loss in obesity. *J Appl*
1674 *Physiol* (1985) 103:21-7.
- 1675 Menshikova EV, Ritov VB, Toledo FG, Ferrell RE, Goodpaster BH, Kelley DE (2005) Effects of weight loss
1676 and physical activity on skeletal muscle mitochondrial function in obesity. *Am J Physiol Endocrinol Metab*
1677 288:E818-25.
- 1678 Miller GA (1991) *The science of words*. Scientific American Library New York:276 pp.
- 1679 Mitchell P (1961) Coupling of phosphorylation to electron and hydrogen transfer by a chemi-osmotic type of
1680 mechanism. *Nature* 191:144-8.
- 1681 Mitchell P (2011) Chemiosmotic coupling in oxidative and photosynthetic phosphorylation. *Biochim Biophys*
1682 *Acta Bioenergetics* 1807:1507-38.
- 1683 Mogensen M, Sahlin K, Fernström M, Glintborg D, Vind BF, Beck-Nielsen H, Højlund K (2007) Mitochondrial
1684 respiration is decreased in skeletal muscle of patients with type 2 diabetes. *Diabetes* 56:1592-9.
- 1685 Mohr PJ, Phillips WD (2015) Dimensionless units in the SI. *Metrologia* 52:40-7.
- 1686 Moreno M, Giacco A, Di Munno C, Goglia F (2017) Direct and rapid effects of 3,5-diiodo-L-thyronine (T2).
1687 *Mol Cell Endocrinol* 7207:30092-8.
- 1688 Morrow RM, Picard M, Derbeneva O, Leipzig J, McManus MJ, Gousspillou G, Barbat-Artigas S, Dos Santos C,
1689 Hepple RT, Murdock DG, Wallace DC (2017) Mitochondrial energy deficiency leads to hyperproliferation of
1690 skeletal muscle mitochondria and enhanced insulin sensitivity. *Proc Natl Acad Sci U S A* 114:2705-10.
- 1691 Murley A, Nunnari J (2016) The emerging network of mitochondria-organelle contacts. *Mol Cell* 61:648-53.
- 1692 National Academies of Sciences, Engineering, and Medicine (2018) *International coordination for science data*
1693 *infrastructure: Proceedings of a workshop—in brief*. Washington, DC: The National Academies Press. doi:
1694 <https://doi.org/10.17226/25015>.
- 1695 Palmfeldt J, Bross P (2017) Proteomics of human mitochondria. *Mitochondrion* 33:2-14.
- 1696 Paradies G, Paradies V, De Benedictis V, Ruggiero FM, Petrosillo G (2014) Functional role of cardiolipin in
1697 mitochondrial bioenergetics. *Biochim Biophys Acta* 1837:408-17.
- 1698 Pesta D, Gnaiger E (2012) High-Resolution Respirometry. OXPHOS protocols for human cells and
1699 permeabilized fibres from small biopsies of human muscle. *Methods Mol Biol* 810:25-58.
- 1700 Pesta D, Hoppel F, Macek C, Messner H, Faulhaber M, Kobel C, Parson W, Burtcher M, Schocke M, Gnaiger
1701 E (2011) Similar qualitative and quantitative changes of mitochondrial respiration following strength and
1702 endurance training in normoxia and hypoxia in sedentary humans. *Am J Physiol Regul Integr Comp Physiol*
1703 301:R1078–87.
- 1704 Price TM, Dai Q (2015) The role of a mitochondrial progesterone receptor (PR-M) in progesterone action.
1705 *Semin Reprod Med* 33:185-94.
- 1706 Puchowicz MA, Varnes ME, Cohen BH, Friedman NR, Kerr DS, Hoppel CL (2004) Oxidative phosphorylation
1707 analysis: assessing the integrated functional activity of human skeletal muscle mitochondria – case studies.
1708 *Mitochondrion* 4:377-85. Puntschart A, Claassen H, Jostardt K, Hoppeler H, Billeter R (1995) mRNAs of

- 1709 enzymes involved in energy metabolism and mtDNA are increased in endurance-trained athletes. *Am J*
 1710 *Physiol* 269:C619-25.
- 1711 Quiros PM, Mottis A, Auwerx J (2016) Mitonuclear communication in homeostasis and stress. *Nat Rev Mol*
 1712 *Cell Biol* 17:213-26.
- 1713 Rackham O, Mercer TR, Filipovska A (2012) The human mitochondrial transcriptome and the RNA-binding
 1714 proteins that regulate its expression. *WIREs RNA* 3:675-95.
- 1715 Reichmann H, Hoppeler H, Mathieu-Costello O, von Bergen F, Pette D (1985) Biochemical and ultrastructural
 1716 changes of skeletal muscle mitochondria after chronic electrical stimulation in rabbits. *Pflügers Arch* 404:1-
 1717 9.
- 1718 Renner K, Amberger A, Konwalinka G, Gnaiger E (2003) Changes of mitochondrial respiration, mitochondrial
 1719 content and cell size after induction of apoptosis in leukemia cells. *Biochim Biophys Acta* 1642:115-23.
- 1720 Rice DW, Alverson AJ, Richardson AO, Young GJ, Sanchez-Puerta MV, Munzinger J, Barry K, Boore JL,
 1721 Zhang Y, dePamphilis CW, Knox EB, Palmer JD (2016) Horizontal transfer of entire genomes via
 1722 mitochondrial fusion in the angiosperm *Amborella*. *Science* 342:1468-73.
- 1723 Rich P (2003) Chemiosmotic coupling: The cost of living. *Nature* 421:583.
- 1724 Rostovtseva TK, Sheldon KL, Hassanzadeh E, Monge C, Saks V, Bezrukov SM, Sackett DL (2008) Tubulin
 1725 binding blocks mitochondrial voltage-dependent anion channel and regulates respiration. *Proc Natl Acad Sci*
 1726 *USA* 105:18746-51.
- 1727 Rustin P, Parfait B, Chretien D, Bourgeron T, Djouadi F, Bastin J, Rötig A, Munnich A (1996) Fluxes of
 1728 nicotinamide adenine dinucleotides through mitochondrial membranes in human cultured cells. *J Biol Chem*
 1729 271:14785-90.
- 1730 Saks VA, Veksler VI, Kuznetsov AV, Kay L, Sikk P, Tiivel T, Tranqui L, Olivares J, Winkler K, Wiedemann F,
 1731 Kunz WS (1998) Permeabilised cell and skinned fiber techniques in studies of mitochondrial function in
 1732 vivo. *Mol Cell Biochem* 184:81-100.
- 1733 Salabei JK, Gibb AA, Hill BG (2014) Comprehensive measurement of respiratory activity in permeabilized cells
 1734 using extracellular flux analysis. *Nat Protoc* 9:421-38.
- 1735 Sazanov LA (2015) A giant molecular proton pump: structure and mechanism of respiratory complex I. *Nat Rev*
 1736 *Mol Cell Biol* 16:375-88.
- 1737 Schneider TD (2006) Claude Shannon: biologist. The founder of information theory used biology to formulate
 1738 the channel capacity. *IEEE Eng Med Biol Mag* 25:30-3.
- 1739 Schönfeld P, Dymkowska D, Wojtczak L (2009) Acyl-CoA-induced generation of reactive oxygen species in
 1740 mitochondrial preparations is due to the presence of peroxisomes. *Free Radic Biol Med* 47:503-9.
- 1741 Schultz J, Wiesner RJ (2000) Proliferation of mitochondria in chronically stimulated rabbit skeletal muscle--
 1742 transcription of mitochondrial genes and copy number of mitochondrial DNA. *J Bioenerg Biomembr* 32:627-
 1743 34.
- 1744 Speijer D (2016) Being right on Q: shaping eukaryotic evolution. *Biochem J* 473:4103-27.
- 1745 Sugiura A, Mattie S, Prudent J, McBride HM (2017) Newly born peroxisomes are a hybrid of mitochondrial and
 1746 ER-derived pre-peroxisomes. *Nature* 542:251-4.
- 1747 Simson P, Jephthina N, Laasmaa M, Peterson P, Birkedal R, Vendelin M (2016) Restricted ADP movement in
 1748 cardiomyocytes: Cytosolic diffusion obstacles are complemented with a small number of open mitochondrial
 1749 voltage-dependent anion channels. *J Mol Cell Cardiol* 97:197-203.
- 1750 Stucki JW, Ineichen EA (1974) Energy dissipation by calcium recycling and the efficiency of calcium transport
 1751 in rat-liver mitochondria. *Eur J Biochem* 48:365-75.
- 1752 Tonkonogi M, Harris B, Sahlin K (1997) Increased activity of citrate synthase in human skeletal muscle after a
 1753 single bout of prolonged exercise. *Acta Physiol Scand* 161:435-6.
- 1754 Torralba D, Baixauli F, Sánchez-Madrid F (2016) Mitochondria know no boundaries: mechanisms and functions
 1755 of intercellular mitochondrial transfer. *Front Cell Dev Biol* 4:107. eCollection 2016.
- 1756 Vamecq J, Schepers L, Parmentier G, Mannaerts GP (1987) Inhibition of peroxisomal fatty acyl-CoA oxidase by
 1757 antimycin A. *Biochem J* 248:603-7.
- 1758 Waczulikova I, Habodaszova D, Cagalinec M, Ferko M, Ulicna O, Mateasik A, Sikurova L, Ziegelhöffer A
 1759 (2007) Mitochondrial membrane fluidity, potential, and calcium transients in the myocardium from acute
 1760 diabetic rats. *Can J Physiol Pharmacol* 85:372-81.
- 1761 Wagner BA, Venkataraman S, Buettner GR (2011) The rate of oxygen utilization by cells. *Free Radic Biol Med*
 1762 51:700-712.
- 1763 Wang H, Hiatt WR, Barstow TJ, Brass EP (1999) Relationships between muscle mitochondrial DNA content,
 1764 mitochondrial enzyme activity and oxidative capacity in man: alterations with disease. *Eur J Appl Physiol*
 1765 *Occup Physiol* 80:22-7.
- 1766 Watt IN, Montgomery MG, Runswick MJ, Leslie AG, Walker JE (2010) Bioenergetic cost of making an
 1767 adenosine triphosphate molecule in animal mitochondria. *Proc Natl Acad Sci U S A* 107:16823-7.
- 1768 Weibel ER, Hoppeler H (2005) Exercise-induced maximal metabolic rate scales with muscle aerobic capacity. *J*
 1769 *Exp Biol* 208:1635-44.

- 1770 White DJ, Wolff JN, Pierson M, Gemmell NJ (2008) Revealing the hidden complexities of mtDNA inheritance.
1771 Mol Ecol 17:4925–42.
- 1772 Wikström M, Hummer G (2012) Stoichiometry of proton translocation by respiratory complex I and its
1773 mechanistic implications. Proc Natl Acad Sci U S A 109:4431-6.
- 1774 Williams EG, Wu Y, Jha P, Dubuis S, Blattmann P, Argmann CA, Houten SM, Amariuta T, Wolski W,
1775 Zamboni N, Aebersold R, Auwerx J (2016) Systems proteomics of liver mitochondria function. Science 352
1776 (6291):aad0189
- 1777 Willis WT, Jackman MR, Messer JI, Kuzmiak-Glancy S, Glancy B (2016) A simple hydraulic analog model of
1778 oxidative phosphorylation. Med Sci Sports Exerc 48:990-1000.
- 1779